

This is a postprint version of the following published document:

Mao, X., Ruiz, E., & Veiga, H. (2017). Threshold stochastic volatility: Properties and forecasting. *International Journal of Forecasting*, 33 (4), pp. 1105-1123.

DOI:[10.1016/j.ijforecast.2017.07.001](https://doi.org/10.1016/j.ijforecast.2017.07.001)

© Elsevier, 2017



This work is licensed under a [Creative Commons Attribution-NonCommercial-NoDerivatives 4.0 International License](https://creativecommons.org/licenses/by-nc-nd/4.0/).

Threshold stochastic volatility: Properties and forecasting

Xiuping Mao^a, Esther Ruiz^{b,c,*}, Helena Veiga^{b,c,d}

^a School of Finance, Zhongnan University of Economics and Law, China

^b Department of Statistics, Universidad Carlos III de Madrid, Spain

^c Instituto Flores de Lemus, Universidad Carlos III de Madrid, Spain

^d BRU-IUL, Instituto Universitario de Lisboa, Portugal

A B S T R A C T

Keywords:

Conditional heteroscedasticity

Leverage effect

MCMC estimator

Option pricing

Volatility forecasting

We analyze the ability of Threshold Stochastic Volatility (TSV) models to represent and forecast asymmetric volatilities. First, we derive the statistical properties of TSV models. Second, we demonstrate the good finite sample properties of a MCMC estimator, implemented in the software package WinBUGS, when estimating the parameters of a general specification, denoted CTSV, that nests the TSV and asymmetric autoregressive stochastic volatility (A-ARSV) models. The MCMC estimator also discriminates between the two specifications and allows us to obtain volatility forecasts. Third, we analyze daily S&P 500 and FTSE 100 returns and show that the estimated CTSV model implies plug-in moments that are slightly closer to the observed sample moments than those implied by other nested specifications. Furthermore, different asymmetric specifications generate rather different European options prices. Finally, although none of the models clearly emerge as best out-of-sample, it seems that including both threshold variables and correlated errors may be a good compromise.

1. Introduction

Stochastic volatility (SV) models are a popular choice for representing the second-order dynamics of financial returns. These models have been generalized to capture the *leverage effect* that is characterized by the asymmetric responses of volatility to positive and negative past returns of the same magnitude; see [Black \(1976\)](#), who was the first to introduce the term ‘leverage effect’. One of these generalizations is the threshold stochastic volatility (TSV) model proposed by [Breidt \(1996\)](#) and [So, Li, and Lam \(2002\)](#), which incorporates the leverage effect by allowing the parameters of the log-volatility equation to differ depending on the sign of the lagged returns. TSV models are quite a popular choice for representing the volatility of financial returns; see, among others, [Asai and McAleer \(2004, 2005, 2011\)](#), [Chen, Liu, and So \(2008, 2013\)](#), [Chen, So, and](#)

[Liu \(2011\)](#), [Elliott, Liew, and Siu \(2011\)](#), [Fan and Wang \(2013\)](#), [Ghosh, Gurung, and Source \(2015\)](#), [Liu, Wong, An, and Zhang \(2014\)](#), [Montero-Lorenzo, Fernández-Avilés, and García-centeno \(2010\)](#), [Muñoz, Marquez, and Acosta \(2007\)](#), [Smith \(2009\)](#), [So and Choi \(2008, 2009\)](#), [Tsai-Hung and Wang \(2013\)](#), [Wu and Zhou \(2015\)](#), [Wirjanto, Kolkiewicz, and Men \(2016\)](#), and [Xu \(2012\)](#). However, to the best of our knowledge, the statistical properties of TSV models are unknown, which makes it difficult to assess their advantages and limitations relative to alternative specifications of the leverage. In particular, it would be interesting to compare TSV models with the popular asymmetric autoregressive SV (A-ARSV) model of [Harvey and Shephard \(1996\)](#) and [Taylor \(1994\)](#), which captures the leverage effect through the correlation between the level and log-volatility disturbances. Given that the properties of TSV models are unknown, only empirical comparisons between these models and alternatives have been carried out. For example, [Asai and McAleer \(2005\)](#) fit TSV and A-ARSV models to four data sets of financial returns and

* Correspondence to: C/ Madrid, 126, 28903, Getafe, Madrid, Spain.
E-mail address: ortega@est-econ.uc3m.es (E. Ruiz).

conclude that the latter model is superior to the former according to both the AIC and the BIC. Similarly, [Smith \(2009\)](#) compares the two models empirically using the same two criteria plus the [Vuong \(1989\)](#) test, and rejects the TSV model in favour of the A-ARSV model for continuously compounded returns on the value-weighted CRSP portfolio. [Wang \(2012\)](#) also compares the TSV model empirically with the asymmetric SV model proposed by [Asai and McAleer \(2005\)](#), in order to consider different distributions for standardized returns, and concludes that the A-ARSV model has a better fit. Finally, [Wu and Zhou \(2015\)](#) find very weak evidence in favour of a TSV specification.

Results on the forecasting performances of TSV models are also scarce. It is important to analyze the similarities and differences between the volatilities predicted using TSV and A-ARSV models, given the implications for practitioners of having an inadequate specification of the asymmetric response of the volatility. In particular, [Christie \(1982\)](#) shows that equity variances have a strong positive association with both financial leverage and interest rates. Furthermore, different specifications of the leverage lead to different formulae for option pricing, meaning that a misspecification of the leverage might result in incorrect option prices; see [Yu, Yang, and Zhang \(2006\)](#). The specification of the leverage effect may also have consequences for financial prices. For example, [Brooks, Henry, and Persaud \(2002\)](#) and [Lien \(2005\)](#) examine its effect on optimal hedge ratios, while [Brooks and Persaud \(2003\)](#) consider its impact on the Value-at-Risk (VaR), and [Pardo and Torro \(2007\)](#) explore its potential for profitable holding strategies.

This paper contributes to the literature on asymmetric SV models in three ways. First, we analyze the ability of TSV models to explain the empirical properties that are usually observed with time series of real financial returns, namely excess kurtosis, positive autocorrelations of squares, and negative cross-correlations between returns and future squared returns. We derive closed-form expressions of these moments when the errors have a generalized error distribution (GED), and the constant and variance of the log-volatility noise change depending on whether past returns are smaller or larger than a given threshold. When the autoregressive parameter changes with past returns, we obtain the statistical properties by simulation. We show that the TSV model captures asymmetric conditional heteroscedasticity if the constant of the log-volatility equation changes. If the persistence parameter also changes, the TSV model can generate moments that are close to those that we usually observe when dealing with high frequency financial returns. However, changes in the variance of the log-volatility noise generate series without leverage. We compare the properties of the TSV and A-ARSV models and show that the former generate slightly less leverage than the latter for particular combinations of the parameters.

The second contribution of this paper is to analyze the finite sample performances of Markov chain Monte Carlo (MCMC) estimators of the parameters of TSV and A-ARSV models with GED errors. Although more efficient MCMC estimators exist, we consider the Bayesian software package WinBUGS based on the single-update Gibbs sampler, as described by [Meyer and Yu \(2000\)](#), due to its ease of

implementation. We show that it has a good finite sample performance and allows us to discriminate among alternative asymmetric specifications. Furthermore, the MCMC estimator also permits the computation of one-step-ahead volatility forecasts.

Our third contribution is an empirical comparison of the TSV and A-ARSV models fitted to daily S&P 500 and FTSE 100 returns. We show that the estimated SV models with both threshold variables and correlated errors imply plug-in moments that are slightly closer to the observed sample moments than those of models which incorporate leverage through either threshold or correlation. The in-sample volatilities estimated by TSV and A-ARSV models generate rather different European option price, meaning that it is important to fit appropriate specifications of the leverage. Finally, although none of the models emerges as clearly the best in the out-of-sample period, it seems that models that include both threshold and correlation may be a good compromise.

The rest of this paper is organized as follows. Section 2 describes the TSV model and derives its analytical properties when the persistence parameter is fixed. Simulations are carried out in order to analyze its properties when the persistence parameter changes. We also compare the statistical properties of the TSV model with those of the A-ARSV model. Section 3 carries out Monte Carlo experiments analyzing the finite sample properties of the MCMC estimator. Section 4 compares the empirical differences among the models in terms of implied plug-in moments, the pricing of European options and the forecasting of volatility in the context of daily S&P 500 and FTSE 100 returns. Finally, Section 5 concludes the paper.

2. Moments of the threshold SV model

This section describes the TSV model and derives its statistical properties.

2.1. The TSV model

Consider the following TSV model:

$$y_t = \exp(h_t/2)\epsilon_t, \quad (1)$$

$$h_t = \begin{cases} \alpha + \phi h_{t-1} + \sigma_\eta \eta_{t-1}, & \epsilon_{t-1} \geq \delta, \\ \alpha + \alpha_0 + (\phi + \phi_0)h_{t-1} + (\sigma_\eta + \sigma_{\eta_0})\eta_{t-1}, & \epsilon_{t-1} < \delta, \end{cases} \quad (2)$$

where y_t is the return at time t , $\sigma_t \equiv \exp(h_t/2)$ is its volatility, η_t is a standardized Gaussian white noise process, and ϵ_t is an independent and identically distributed sequence with mean zero and variance one that is independent of η_t for all leads and lags. The TSV model incorporates the leverage effect by allowing the parameters of the log-volatility equation to change depending on whether past standardized returns are smaller or larger than the threshold δ .

Several restricted versions of the TSV model in Eqs. (1) and (2) have been considered previously in the literature. For example, [Wirjanto et al. \(2016\)](#) consider a TSV model with $\phi_0 = \sigma_{\eta_0} = 0$ and ϵ_t being Gaussian. [Asai and McAleer \(2004\)](#) further assume that $\delta = 0$. Several other authors also assume that $\delta = 0$ and ϵ_t are Gaussian; see for example [Breidt \(1996\)](#), as well as [Lien \(2005\)](#), who further

considers $\alpha_0 = \sigma_{\eta_0} = 0$. Finally, [Wang \(2012\)](#) assumes $\delta = 0$ and ϵ_t having a generalized- t distribution, while [So et al. \(2002\)](#) consider a TSV model with $\delta = \sigma_{\eta_0} = 0$.

On the other hand, the TSV model has also been extended in several directions. For example, [Chen et al. \(2008, 2013\)](#) account for uncertainty in the unobserved time-delay parameter of the threshold variable. They assume that ϵ_t has a standardized Student- t distribution, and consider both self-exciting and exogenous threshold variables. However, [Chen et al. \(2013\)](#) point out the difficulties associated with the selection of exogenous threshold variables, and this paper therefore focuses on self-exciting models. When estimating self-exciting models, the delay parameter is often assumed to be one, and this is the case that we will consider from now on; see [Chen et al. \(2008, 2013\)](#). Finally, several authors have also considered thresholds in the parameters of the conditional mean; see for example [Chen et al. \(2008, 2013\)](#), [So et al. \(2002\)](#) and [Wu and Zhou \(2015\)](#). However, the estimated parameters of the conditional mean in these papers are either non-significant or too small. Thus, this paper focuses on the specification of the conditional volatility, assuming a zero conditional mean. When $\delta = 0$, the TSV model in Eqs. (1) and (2) has also been extended to include the correlation between ϵ_t and η_t ; see for instance [Asai and McAleer \(2004\)](#), [Smith \(2009\)](#), [Wu and Zhou \(2015\)](#) and [Xu \(2010\)](#). These two latter works further assume that the correlation switches between the two regimes according to the lagged return sign. The SV model in which the leverage effect is represented by both the use of different parameters depending on whether or not past standardized returns are above a given threshold and the inclusion of the correlation between ϵ_t and η_t is referred to as the correlated TSV (CTSV) model, and is given by Eq. (1), where h_t is defined as

$$h_t = (\phi + \phi_0 I(\epsilon_{t-1} < \delta)) h_{t-1} + f(\epsilon_{t-1}, \eta_{t-1}; \theta), \quad (3)$$

where

$$f(\epsilon_{t-1}, \eta_{t-1}; \theta) = \alpha + \alpha_0 I(\epsilon_{t-1} < \delta) + \gamma_1 \epsilon_{t-1} + (\sigma_\eta + \sigma_{\eta_0} I(\epsilon_{t-1} < \delta)) \eta_{t-1}. \quad (4)$$

Note that the popular asymmetric autoregressive log-volatility model, denoted as A-ARSV and proposed by [Harvey and Shephard \(1996\)](#) and [Taylor \(1994\)](#), is obtained when $\alpha_0 = \phi_0 = \sigma_{\eta_0} = 0$; see [Asai and McAleer \(2011\)](#) and [Yu \(2012\)](#) for the equivalence of this specification to that where the leverage effect is captured through the correlation between the level and volatility noises when ϵ_t is a standard Gaussian white noise process.

The alternative TSV model specifications that we described above have often been fitted to real time series of returns without any explicit reference to the moments that they can represent. For example, analytical expressions of the statistical properties of the A-ARSV model are derived by [Demos \(2002\)](#), [Mao, Ruiz, Veiga, and Czellar \(2015\)](#), [Pérez, Ruiz, and Veiga \(2009\)](#), [Ruiz and Veiga \(2008\)](#) and [Taylor \(2007, 1994\)](#), who consider a range of different assumptions about the probability distribution of ϵ_t . However, as far as we know, there are no results available on

the moments of the TSV model.¹ It is important to note that the derivation of the moments of TSV models in which the autoregressive parameter changes is subject to technical difficulties, given that the conditions on the autoregressive parameters that guarantee the stationarity of the process are not clear. Consequently, Section 2.2 derives analytical expressions of several relevant moments of the TSV model in which $\phi_0 = 0$. In particular, we derive the kurtosis, autocorrelations of squared returns and cross-correlations between returns and future squared returns when ϵ_t has a GED distribution with parameter ν , $\text{GED}(\nu)$.² Section 2.3 generates artificial data for obtaining the statistical properties of the TSV model by simulation when $\phi_0 \neq 0$.

2.2. Analytical properties of the TSV model with $\phi_0 = 0$

Consider the TSV model defined in Eqs. (1) and (2) with $\phi_0 = 0$. First of all, note that $\text{Var}(\alpha + \alpha_0 I(\epsilon_{t-1} < \delta) + (\sigma_\eta + \sigma_{\eta_0} I(\epsilon_{t-1} < \delta)) \eta_t) < \infty$, and consequently, y_t is strictly stationary if $|\phi| < 1$; see [Appendix A.1](#) for the proof. Furthermore, the variance and kurtosis of y_t are given by

$$\text{Var}(y_t) = P(1, \phi) \quad (5)$$

and

$$k_y = k_\epsilon \frac{P(2, \phi)}{(P(1, \phi))^2} \quad (6)$$

respectively, where k_ϵ is the kurtosis of ϵ_t and

$$\begin{aligned} P(a, b) &= \prod_{i=1}^{\infty} \left\{ \text{Prob}(\epsilon \geq \delta) \exp\left(\frac{a^2 b^{2(i-1)} \sigma_\eta^2}{2}\right) \exp(ab^{i-1} \alpha) \right. \\ &\quad \left. + \text{Prob}(\epsilon < \delta) \exp\left(\frac{a^2 b^{2(i-1)} (\sigma_\eta + \sigma_{\eta_0})^2}{2}\right) \right. \\ &\quad \left. \times \exp(ab^{i-1} (\alpha + \alpha_0)) \right\}; \end{aligned} \quad (7)$$

see [Appendix A.2](#) for the derivation of the moments of y_t .³ The expression of $\text{Prob}(\epsilon \leq \delta)$ depends on the particular distribution assumed for ϵ_t . It is derived in [Appendix B.1](#) for the case where ϵ_t has a $\text{GED}(\nu)$ distribution. Finally, note that the infinite product needs to be truncated in order to

¹ [García-centeno and Mínguez-Salido \(2009\)](#) derive the moments of the TSV model under the assumption that $\delta = 0$. However, their derivation is based on the incorrect assumption that h_t is a first order stationary autoregressive process. For the same model, [Lien \(2005\)](#) derives the first two moments of the log-volatility when $\alpha_0 = \sigma_{\eta_0} = 0$. [Diop and Guegan \(2004\)](#) consider the TSV model in Eqs. (1) and (2) with $\alpha_0 = 0$, give conditions for strict stationarity of the log-volatility process, and show that the marginal distribution of h_t has Pareto-like tails. However, the moments of y_t are unknown.

² The GED distribution with parameter ν is described by [Harvey \(1990\)](#) and has the advantage that it includes distributions with different tail thicknesses, such as, for example, the normal when $\nu = 2$, the double exponential when $\nu = 1$ and the uniform when $\nu = \infty$. The GED distribution has heavy tails if $\nu < 2$.

³ The moments in [Appendix A.2](#) are derived for the CTSV model in Eqs. (1) and (3). The moments of the TSV model are obtained from the expressions in [Appendix A.2](#) with $\gamma_1 = 0$.

$$\begin{aligned} \rho_2(r) &= \text{corr}(y_t^2, y_{t+r}^2) \\ &= \frac{E(\epsilon_t^2 \exp(\phi^{r-1}(\alpha + \alpha_0 I(\epsilon_t < \delta) + (\sigma_\eta + \sigma_{\eta_0} I(\epsilon_t < \delta))\eta_t)))P((1 + \phi^r), \phi)Q_r(1, \phi) - (P(1, \phi))^2}{k_\epsilon P(2, \phi) - (P(1, \phi))^2}, \end{aligned} \quad (8)$$

Box I.

$$\rho_{21}(r) = \frac{E(\epsilon_t \exp(\phi^{r-1}(\alpha + \alpha_0 I(\epsilon_t < \delta) + (\sigma_\eta + \sigma_{\eta_0} I(\epsilon_t < \delta))\eta_t)))P(0.5(1 + 2\phi^r), \phi)Q_r(1, \phi)}{\sqrt{P(1, \phi)(k_\epsilon P(2, \phi) - (P(1, \phi))^2)}}; \quad (9)$$

Box II.

compute $P(\cdot, \cdot)$. Our experience suggests that stable results can be obtained by truncating it at $i = 500$. For general distributions of ϵ_t , the probabilities required to compute Eq. (7) can be obtained by simulation.

We illustrate the values of the kurtosis of returns in Eq. (6) by considering a TSV model given by Eqs. (1) and (2) with $\epsilon_t \sim N(0, 1)$, $\phi = 0.98$, $\sigma_\eta^2 = 0.05$, $\phi_0 = \sigma_{\eta_0} = \delta = 0$, while the constant is allowed to change according to the following combinations $\{\alpha, \alpha + \alpha_0\} = \{-0.12, 0.08\}$, $\{-0.07, 0.05\}$ and $\{-0.14, 0.1\}$, which are chosen to resemble the parameter values that are often obtained when the TSV model is fitted to real data; see [Asai and McAleer \(2004\)](#), [So et al. \(2002\)](#), and [Xu \(2012\)](#). These models are denoted by M1, M2 and M3, respectively. Their kurtoses, reported in [Table 1](#), are similar to those that are often observed when dealing with real financial returns; see for example the sample kurtosis of S&P 500 returns reported in [Table 3](#), which is 11.009. We also consider models in which $\alpha = \alpha_0 = 0$ and $\phi = 0.98$, while the variance of the log-volatility noise changes according to the combinations $\{\sigma_\eta^2, (\sigma_\eta + \sigma_{\eta_0})^2\} = \{0.05, 0.04\}$ and $\{0.05, 0.02\}$. These models are denoted M4 and M5, respectively. Again, the kurtoses reported in [Table 1](#) are close to those obtained with real time series of financial returns, though they are slightly smaller than those obtained for models M1, M2 and M3. We illustrate the properties when $\delta \neq 0$ by considering two additional TSV models with $\delta = -0.4$, denoted M6 and M7, with the parameter values reported in [Table 1](#). We can observe that the kurtoses of returns are very similar to those of the corresponding TSV models with $\delta = 0$.

With respect to the temporal dependence of returns, it is easy to prove that they are a martingale difference, though not an independent sequence. When $|\phi| < 1$, the r th order autocorrelation of y_t^2 for $r > 0$ is given by [Box I](#), where $Q_1(a, b) \equiv 1$ and $Q_n(a, b) \equiv \prod_{i=1}^{n-1} E(\exp(ab^{i-1}(\alpha + \alpha_0 I(\epsilon_t < \delta) + (\sigma_\eta + \sigma_{\eta_0} I(\epsilon_t < \delta))\eta_t)))$ if $n > 1$; see [Appendix A.3](#) for the autocorrelation of y_t^c for any positive integer c . The expectations that are required for computing Eq. (8) when ϵ_t follows a GED(ν) distribution are derived in [Appendix B.2](#).⁴

⁴ Once again, [Appendix B.2](#) derives the expectations for $f(\epsilon_t, \eta_t; \theta) \equiv \alpha + \alpha_0 I(\epsilon_t < \delta) + \gamma_1 \epsilon_t + (\sigma_\eta + \sigma_{\eta_0} I(\epsilon_t < \delta))\eta_t$. To obtain the required expectations, set $\gamma_1 = 0$.

[Table 1](#) reports the first order autocorrelations of squares for the models described above. We can see that the value of α_0 has barely any influence on the autocorrelations of squares. The first order autocorrelations of squares of models M1, M2 and M3 are indistinguishable. The corresponding autocorrelations of models M4 and M5, in which the constant is fixed and the variance of the log-volatility, σ_η^2 , changes, are slightly lower, meaning that the conditional heteroscedasticity is weaker when the variance is not constant. Note that the autocorrelations of squares decrease as the difference between the variances in the two regimes increases. Finally, when the threshold is $\delta = -0.4$, the TSV model generates returns with autocorrelations of squares that are similar to those of the corresponding TSV model with $\delta = 0$.

The leverage effect is reflected in the negative cross-correlations between returns and future squared returns. When $|\phi| < 1$, the expression of the r th order cross-correlation between y_t and y_{t+r}^2 for $r > 0$ is given by [Box II](#), see [Appendix A.4](#) for the derivation. The expectation involved in the numerator of Eq. (9) has been derived in [Appendix B.2](#) for the case where ϵ_t has a GED(ν) distribution. The first order cross-correlations for the TSV models considered above are reported in [Table 1](#). We observe that larger values of α_0 generate returns with a stronger leverage effect. Therefore, changes in the constant of the log-volatility equation capture the leverage effect without destroying the conditional heteroscedasticity. Regarding the corresponding cross-correlations of models M4 and M5, in which the variance of η_t changes in both regimes, we observe that their magnitudes are nearly zero. Therefore, changes in the variance of the noise of the log-volatility generate conditional heteroscedasticity without the leverage effect. As a consequence, we will focus on TSV models with $\sigma_{\eta_0} = 0$ from now on. On the other hand, the correlations when $\delta = -0.4$ are very similar to the corresponding TSV models with $\delta = 0$. Consequently, we can conclude that the particular value of the threshold does not affect the statistical properties of TSV models when ϕ is fixed.

The asymmetric response of the volatility to shocks in the level and in the volatility for a TSV model can be obtained as

$$V = \sigma_y^{2(\phi + \phi_0 I(\epsilon < \delta))} \exp(f(\epsilon, \eta; \theta)), \quad (10)$$

where σ_y^2 is the marginal variance of y_t given by Eq. (5). As an illustration, [Fig. 1](#) plots this function for a TSV model

Table 1

Theoretical (upper panel) and Monte Carlo means and standard deviations (in parentheses; lower panel) of the sample kurtosis, first order autocorrelation of squares and first order cross-correlation of CTSV models.

Model	α	$\alpha + \alpha_0$	ϕ	$\phi + \phi_0$	σ_η^2	$(\sigma_\eta + \sigma_{\eta_0})^2$	γ_1	δ	Kurtosis	$\rho_2(1)$	$\rho_{21}(1)$
M1	-0.12	0.08	0.98		0.05		0	0	13.630	0.270	-0.039
M2	-0.07	0.05	0.98		0.05		0	0	11.611	0.261	-0.024
M3	-0.14	0.1	0.98		0.05		0	0	15.208	0.275	-0.046
M4	0		0.98		0.05	0.04	0	0	9.352	0.245	0.001
M5	0		0.98		0.05	0.02	0	0	7.297	0.221	0.003
M6	-0.12	0.08	0.98		0.05		0	-0.4	13.435	0.280	-0.040
M7	0		0.98		0.05	0.04	0	-0.4	9.725	0.248	0.001
M8	0		0.95	0.98	0.05		0	0	6.233 (0.441)	0.196 (0.018)	-0.007 (0.009)
M9	-0.12	0.08	0.95	0.98	0.05		0	0	8.192 (1.343)	0.226 (0.026)	-0.055 (0.012)
M10	-0.12	0.08	0.95	0.98	0.05		0	-0.4	6.229 (1.369)	0.205 (0.048)	-0.042 (0.029)
M11	-0.12	0.08	0.95	0.98	0.05		-0.07	0	9.415 (3.799)	0.235 (0.061)	-0.082 (0.034)
M12	-0.12	0.08	0.95	0.98	0.05		-0.07	-0.4	7.713 (2.132)	0.229 (0.054)	-0.078 (0.032)

with parameters $\phi = 0.98$, $\sigma_\eta^2 = 0.05$, $\alpha_0 = 0.2$ and $\phi_0 = \sigma_{\eta_0} = \delta = 0$. The value of α is chosen such that $\exp(\alpha)\sigma_y^{2\phi} = 1$. The main characteristic of the volatility response plotted in Fig. 1 is its discontinuity with respect to ϵ . Furthermore, it is important to point out that the volatility response plotted in Fig. 1 represents different leverage effects depending on the value of the log-volatility disturbance. The volatility response to the return error, ϵ , depends on the volatility error, η : it is less asymmetric in tranquil periods, when η is negative, than in periods of turmoil, when η is positive. Note that Clark (1973) proposes SV models for prices which assume that they evolve at different rates during identical time intervals (days). The differences in the evolution of prices on different days can be attributed to the fact that the rate at which information is available to traders varies. On days when no new information is available, trading is slow and prices evolve slowly. According to Fig. 1, the leverage effect is smaller on these days than on days in which new information appears in the market. In the latter case, trading is brisk and prices evolve much faster. Finally, note that, given η_t , the response to different values of the level disturbance, ϵ_t , within each regime, does not depend on ϵ_t . The volatility increases more after negative returns, but this increase is independent of the size of the level shocks to returns.

2.3. Simulated moments of the TSV model with varying persistence

This subsection analyzes the statistical properties of the TSV model when the autoregressive parameter of the log-volatility equation changes depending on whether the lagged standardized returns are larger or smaller than the threshold. As was mentioned above, it is not possible to obtain analytical moments in this case, and therefore the moments are obtained by simulation. We consider three models with Gaussian errors. Note that, according to the results of Mao et al. (2015), if the errors have a distribution with heavy tails, the magnitudes of both the autocorrelations of squares and the cross-correlations will be smaller than those of the corresponding model with

Gaussian errors. Furthermore, changes in the distribution of ϵ_t affect the autocorrelations of squares more than the cross-correlations. In the first model, denoted M8, $\alpha = \alpha_0 = \delta = 0$ and $\sigma_\eta^2 = 0.05$, while the persistence parameter is $\phi = 0.95$ in the first regime and $\phi + \phi_0 = 0.98$ in the second; see García-centeno and Mínguez-Salido (2009), Lien (2005), Montero-Lorenzo et al. (2010) and Montero-Lorenzo, García-centeno, and Fernández-Avilés (2011) for similar estimates of ϕ and $\phi + \phi_0$. In the second model, denoted M9, all of the parameters are the same except that $\alpha = -0.12$ and $\alpha + \alpha_0 = 0.08$, while in the third model, M10, $\delta = -0.4$.⁵ The sample kurtoses, autocorrelations of squares and cross-correlations between levels and future squares are obtained by simulating $R = 1,000$ series of size $T = 10,000$ from each of these models. Table 1, which reports the Monte Carlo averages and standard deviations of the sample kurtoses and first order autocorrelations of squares, shows that they are smaller than those of the corresponding models with fixed ϕ , and closer to those of financial returns. Furthermore, the Monte Carlo averages of the first order cross-correlations reported in Table 1 show that changes in ϕ that are not coupled with changes in the constant of the log-volatility equation, as in model M8, may not generate asymmetric heteroscedasticity. However, the leverage effect is reinforced if the constant changes. If $\delta = -0.4$, the kurtosis, first order autocorrelation of squares and first order cross-correlation between returns and squared returns all decrease with respect to the model with $\delta = 0$.

Finally, we consider a CTSV model in which the log-volatility is defined as in Eq. (3), with $f(\cdot, \cdot; \cdot)$ defined as in Eq. (4). This model incorporates the leverage effect through both correlation and threshold. Table 1 reports the moments considered above for models M11 and M12, which have the same parameter values as models M9 and M10 respectively, but with $\gamma_1 = -0.07$ instead of $\gamma_1 = 0$.

⁵ We have also conducted more simulations to consider models in which both α and σ_η^2 or all three parameters change simultaneously with the sign of lagged returns, and found that a change in σ_η^2 always decreases the leverage effect. All of the results are available from the authors upon request.

2.4. Threshold versus correlation

This subsection compares the statistical properties of the TSV model with those of the popular A-ARSV model when the errors have a Gaussian distribution; see [Delatola and Griffin \(2013\)](#), [Jensen and Maheu \(2014\)](#), [Skaug and Yu \(2014\)](#) and [Wang, Chan, and Choy \(2013\)](#), for some recent works dealing with A-ARSV models.

We first compare the A-ARSV and TSV models when $\phi_0 = \sigma_{\eta_0} = \delta = 0$. The difference between these two models is the way in which the leverage is incorporated. The A-ARSV model incorporates it through γ_1 , while the TSV model captures it via the α_0 parameter. Heuristically, we observe that the kurtoses generated by the TSV and A-ARSV models for $\gamma_1 = -0.5\alpha_0$ are the same for small values of α ; see the top panel of [Fig. 2](#). On the other hand, [Fig. 2](#) plots the first order autocorrelations of squares and cross-correlations between returns and future squared returns for different combinations of ϕ and σ_{η}^2 in order to check whether the returns generated by the two models with the same kurtoses have similar dynamics. In particular, we choose $(\phi, \sigma_{\eta}^2) = (0.98, 0.02)$, $(0.98, 0.01)$ and $(0.99, 0.01)$. We can see that, for a given kurtosis, the two models generate very similar values of the correlations of squares, regardless of the values of their parameters. However, the A-ARSV model is able to generate returns with larger absolute cross-correlations than those of the TSV model for the same kurtosis and ϕ and σ_{η}^2 parameters.

We also compute the asymmetric volatility response of the A-ARSV model with parameters $\phi = 0.98$ and $\sigma_{\eta}^2 = 0.05$ to level and volatility shocks. In order to ensure that the A-ARSV model is comparable to the TSV model considered in [Fig. 1](#), the value of γ_1 has been chosen to be $\gamma_1 = -0.08$. Comparing the surfaces plotted in the two panels of [Fig. 1](#), we can see that the volatilities of the TSV and A-ARSV models respond quite differently to past level and log-volatility shocks. The response of the A-ARSV model is smoother and, for a given value of the log-volatility shock η , the difference between level shocks of the same magnitude but different signs is larger than in the TSV model, provided that the shock is not very small. Only when ϵ is relatively small is the leverage effect of the TSV model larger than that of the A-ARSV model. These differences may affect the forecasting of volatilities.

3. MCMC estimator

The empirical implementation of SV models for forecasting purposes requires the parameters to be estimated, which is often done based on the evaluation of an analytically intractable likelihood function. The key challenge is the computation of a high dimensional integral. MCMC approaches have become very popular in the context of asymmetric stochastic volatility models, due to their good properties when estimating parameters and volatilities; see for example [Chen et al. \(2008, 2013\)](#), [Liu et al. \(2014\)](#), [Montero-Lorenzo et al. \(2010\)](#), [Montero-Lorenzo et al. \(2011\)](#), [So and Choi \(2009\)](#), [So et al. \(2002\)](#), [Tsai-Hung and](#)

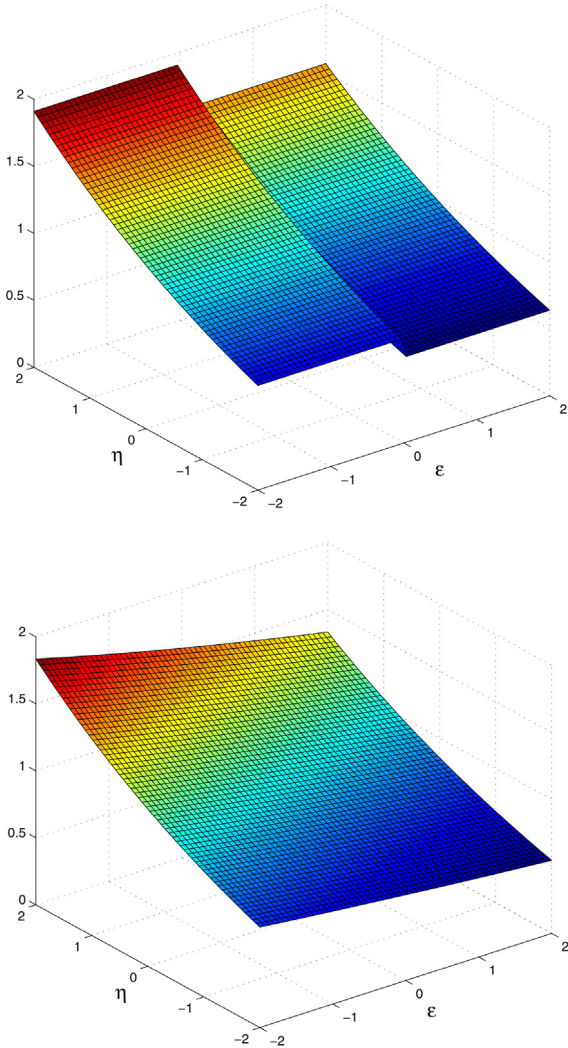


Fig. 1. Asymmetric responses of the volatilities of TSV (upper panel) and A-ARSV (lower panel) models with parameters $\phi = 0.98$, $\sigma_{\eta}^2 = 0.05$, $\phi_0 = \sigma_{\eta_0} = \delta = 0$ and $\exp(\alpha)\sigma_y^{2\phi} = 1$ and leverage parameters $\alpha_0 = 0.2$ and $\gamma_1 = -0.08$, respectively.

As expected, when comparing the moments of the TSV and CTSV models, the latter have larger kurtoses, autocorrelations of squares and cross-correlations than the former.

Summing up, changes in σ_{η}^2 do not capture the leverage effect, while the threshold in the constant of the log-volatility equation enables the TSV model to capture it. Furthermore, models in which the constant and the autoregressive parameter change simultaneously generate series with properties that are similar to those encountered in empirical applications. Incorporating a threshold that is different from zero does not have implications for the moments when ϕ is constant, but when ϕ changes it decreases the kurtosis, the autocorrelations of squares and the cross-correlations. Finally, specifications in which the leverage is modeled using both threshold variables and correlated errors are also appropriate for representing the moments of real financial returns.

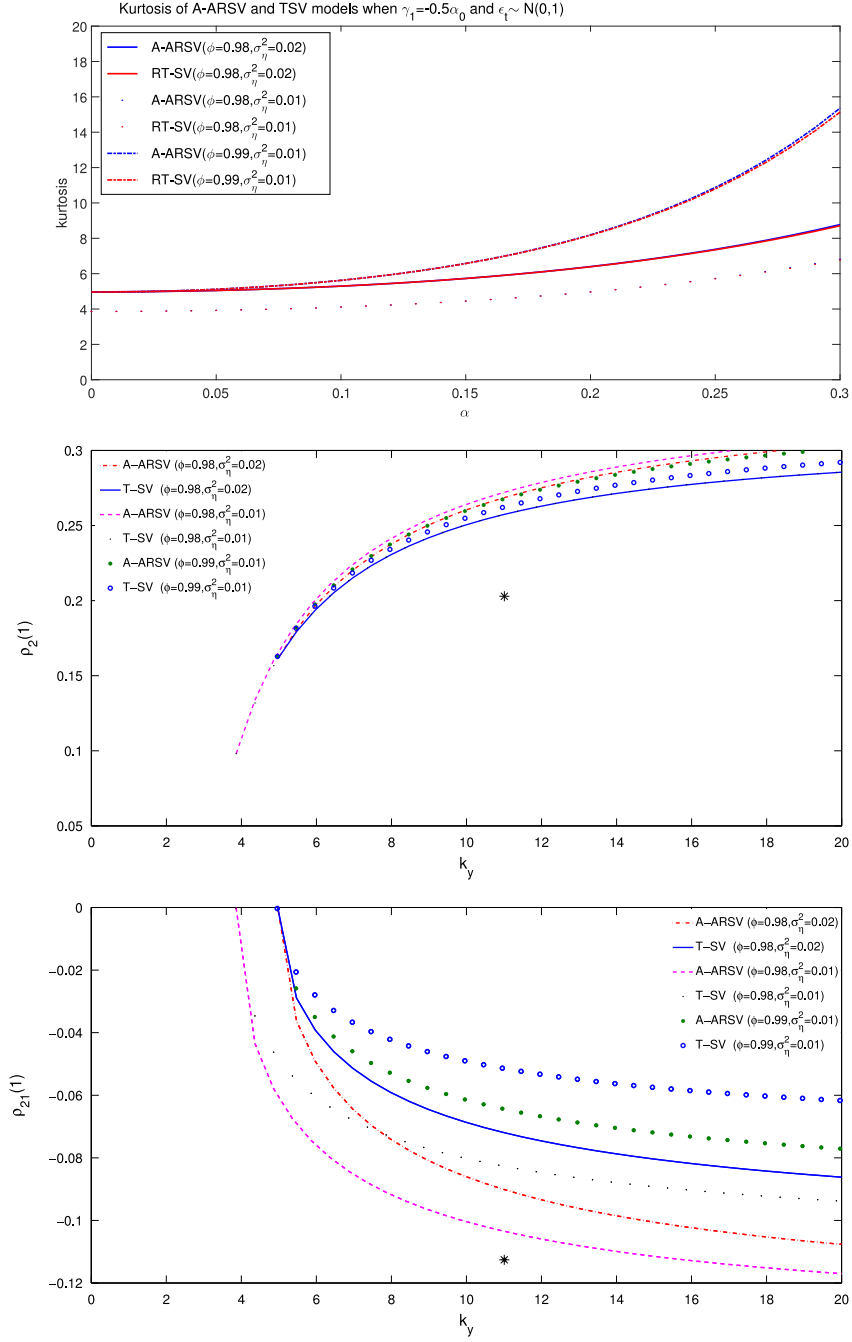


Fig. 2. Relationship between the kurtosis and α in A-ARSV and TSV models (top), first order autocorrelations of squares (centre) and cross-correlations between returns and future squared returns (bottom) in TSV and A-ARSV models with the same kurtosis when $\phi = 0.98$, $\sigma_\eta^2 = 0.02$ (dotted line), $\phi = 0.98$, $\sigma_\eta^2 = 0.01$ (dash-dot line) and $\phi = 0.99$, $\sigma_\eta^2 = 0.01$ (circled line). The stars represent the sample moments of S&P 500 returns.

Wang (2013) and Wang (2012).⁶ This paper considers an MCMC estimator that is implemented in the user-friendly

⁶ Alternatively, Smith (2009) proposes an estimator of the parameters of the CTSV model that is based on evaluating the likelihood function via simulation, extending the ML estimator of Fridman and Harris (1998) and Kitagawa (1987). Other simulated ML estimators, such as the numerically accelerated importance sampling (NAIS) estimator proposed by Koopman, Lucas, and Scharth (2015), for example, can be implemented for

and freely available WinBUGS software described by Meyer and Yu (2000). The estimator is based on a single-move Gibbs sampling algorithm and has been implemented in the context of asymmetric SV models by Smith (2009),

the estimation of TSV models without incorporating correlation. In any case, a comparison of the performances of alternative estimators of the parameters of the CTSV model is beyond the objectives of this paper.

Wang et al. (2013) and Yu (2012), among others. The MCMC estimator implemented in WinBUGS is appealing because it can handle non-Gaussian level disturbances without much programming effort. Furthermore, the WinBUGS estimator allows one-step-ahead volatility forecasts to be obtained by specifying the predicted distribution for the volatility in a similar way to the posterior distribution. The predicted mean volatilities depend on the estimated parameters and on the estimated volatility at the end of the sample.

We carry out Monte Carlo experiments in order to analyze the finite sample performance of the WinBUGS parameter estimator in the context of CTSV models. The nesting CTSV model generates $R = 200$ series of size $T = 1000$ with GED errors and different parameter values; see Table 2 for a description of the models considered. For each replication, the parameters are estimated using the WinBUGS estimator. Table 2 reports the Monte Carlo averages and standard deviations of the estimated parameters, obtained as the means and standard deviations of the posterior distribution, of the general CTSV model when the errors are GED with the parameter $\nu = 1.5$ and a threshold of $\delta = -0.4$. We can see that the parameters in the model have rather small biases and standard deviations even if the sample size is moderate, $T = 1000$, meaning that inference based on the WinBUGS estimator is reliable.

We check whether the WinBUGS estimator is able to identify the source of volatility asymmetry by also generating series which assume that either $\gamma_1 = 0$ or $\delta = 0$, and estimating both parameters. The estimates are not significantly different from zero in either case.

Finally, Table 2 also reports Monte Carlo results of several restricted versions of the CTSV model and shows that the MCMC estimator has adequate finite sample properties to estimate their parameters.

4. Empirical comparison

This section compares the in-sample fits, economic implications for option pricing, and out-of-sample volatility forecasting performances of different restricted CTSV models when they are fitted to daily S&P 500 and FTSE 100 returns observed between January 3, 2000 and January 29, 2015.⁷

4.1. Descriptive analysis and estimation results

The S&P 500 and FTSE 100 returns are plotted in Figs. 3 and 4, respectively. Table 3, which reports the total sample sizes and some summary statistics, shows that both returns are negatively skewed and demonstrate leptokurtosis. Moreover, the significant positive first order autocorrelation of squares and the negative cross-correlation between returns and future squared returns suggest the existence of volatility clustering and a leverage effect; see also the sample autocorrelations and cross-correlations plotted in Figs. 3 and 4.

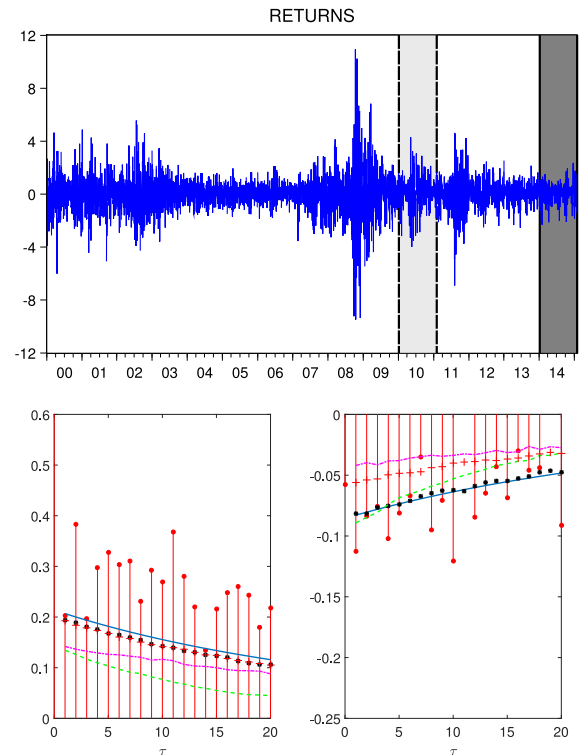


Fig. 3. The top graph displays daily S&P 500 returns, with the vertical line indicating the start of the out-of-sample period. The two shaded areas correspond to the first (dark grey) and second (light grey) out-of-sample periods, respectively. The bottom graphs show the sample autocorrelations of squares (left) and cross-correlations of returns and future squared returns (right), together with the corresponding plug-in moments obtained after fitting the CTSV1 (green dashed lines), CTSV2 (black star-marked lines), A-ARSV (blue continuous lines), TSV1 (magenta dash-dot lines), and TSV2 (red plus-marked lines) models to the daily S&P 500 returns.

A CTSV model is fitted in order to represent the empirical moments and dynamic dependence of the two series of returns that we consider, and its parameters are estimated by WinBUGS, with the autoregressive parameters restricted to be strictly smaller than one in both regimes. After estimating the parameters, we compute the deviance information criterion (DIC) proposed by Berg, Meyer, and Yu (2004), who show that it provides an efficient and straightforward way of identifying the most appropriate model; see the studies by Smith (2009) and Wang (2012), who also use the DIC in the context of SV models. The DIC has been computed using the program WinBUGS based on the conditional likelihood; see Li, Zeng, and Yu (2014) for a description of alternative definitions of the DIC. Note that both the latent volatilities and the parameters are in focus when using the DIC as computed by WinBUGS. On top of the general CTSV model, denoted by CTSV1 in Table 4, we also fit several restricted versions for purposes of comparison. First, we consider the CTSV model in which the threshold is restricted to be zero. This model is denoted by CTSV2. Second, we fit two competing nested models that are usually fitted and compared in the literature, namely the A-ARSV model and the TSV model. In the latter case, we

⁷ The data were collected from the Yahoo Finance website (<http://finance.yahoo.com>).

Table 2
Monte Carlo averages and standard deviations of WinBUGS parameter estimates ($T = 1000$).

	α		ϕ		γ_1	δ	σ_η^2	ν	
	α	α_0	ϕ	ϕ_0					
CTSV	True value	-0.140	0.240	0.900	0.080	-0.070	-0.400	0.020	1.500
	MC average	-0.170	0.259	0.859	0.054	-0.082	-0.436	0.019	1.453
	S.D.	(0.035)	(0.044)	(0.033)	(0.043)	(0.039)	(0.167)	(0.010)	(0.116)
	True value	-0.140	0.240	0.900	0.080	0.000	-0.400	0.020	1.500
	MC average	-0.203	0.265	0.820	0.051	-0.004	-0.433	0.021	1.453
	S.D.	(0.056)	(0.041)	(0.060)	(0.039)	(0.041)	(0.162)	(0.013)	(0.113)
	True value	-0.140	0.240	0.900	0.080	-0.070	0.000	0.020	1.500
	MC average	-0.146	0.247	0.891	0.068	-0.075	-0.011	0.019	1.468
	S.D.	(0.028)	(0.054)	(0.025)	(0.043)	(0.037)	(0.031)	(0.010)	(0.113)
	True value	-0.140	0.240	0.900	0.080	-0.070	0.000	0.020	1.500
	MC average	-0.148	0.251	0.893	0.074	-0.077		0.018	1.464
	S.D.	(0.022)	(0.044)	(0.025)	(0.046)	(0.029)		(0.008)	(0.126)
True value	0.000	0.000	0.980	0.000	-0.070		0.020	1.500	
MC average	0.002	-0.006	0.954	0.024	-0.083		0.026	1.490	
S.D.	(0.029)	(0.058)	(0.019)	(0.030)	(0.029)		(0.010)	(0.130)	
A-ARSV	True value	0.000		0.980		-0.070		0.020	2.000
	MC average	0.000		0.968		-0.075		0.027	2.041
	S.D.	(0.008)		(0.012)		(0.022)		(0.010)	(0.195)
	True value	0.000		0.980		-0.070		0.020	1.500
	MC average	-0.001		0.965		-0.076		0.027	1.505
	S.D.	(0.007)		(0.017)		(0.025)		(0.011)	(0.115)
TSV	True value	-0.140	0.240	0.980				0.020	1.500
	MC average	-0.162	0.255	0.968				0.026	1.471
	S.D.	(0.026)	(0.041)	(0.012)				(0.011)	(0.110)
	True value	-0.140	0.240	0.980				0.010	1.500
	MC average	-0.164	0.258	0.966				0.017	1.476
	S.D.	(0.025)	(0.035)	(0.012)				(0.008)	(0.120)
	True value	-0.140	0.240	0.900	0.080			0.020	1.500
	MC average	-0.149	0.243	0.886	0.073			0.022	1.481
	S.D.	(0.022)	(0.040)	(0.029)	(0.045)			(0.012)	(0.130)
	True value	-0.140	0.240	0.900	0.080			0.010	1.500
MC average	-0.162	0.257	0.872	0.068			0.015	1.510	
S.D.	(0.028)	(0.035)	(0.036)	(0.042)			(0.007)	(0.118)	

Table 3
Sample moments of daily S&P 500 and FTSE 100 mean-adjusted returns.

	S&P 500			FTSE 100		
	Full sample	Out-of-sample		Full sample	Out-of-sample	
		Period 1	Period 2		Period 1	Period 2
Sample size	3792	271	271	3926	274	274
Median	0.049	0.066	0.083	0.0004	0.039	-0.015
Maximum	10.949	2.373	4.303	9.385	2.383	3.071
Minimum	-9.478	-2.310	-3.976	-9.264	-2.874	-3.194
Std. Dev.	1.283	0.745	1.107	1.220	0.756	1.029
Skewness	-0.183	-0.341*	-0.227*	-0.158*	-0.288*	-0.215*
Kurtosis	11.009*	3.924*	5.168*	9.456*	4.727*	3.777*
Jarque-Bera	10154.690	14.888	55.399	6834.150	37.833	8.997
(<i>p</i> -value)	(0.000)	(0.001)	(0.000)	(0.000)	(0.000)	(0.011)
$\rho_2(1)$	0.203*	0.203*	-0.016	0.236*	0.177*	-0.006
$\rho_{21}(1)$	-0.113*	-0.149*	-0.168*	-0.102*	-0.145*	-0.037

* Indicates statistical significance at the 1% level.

consider both a threshold of zero and a non-zero threshold, and denote the corresponding models TSV1 and TSV2, respectively. Finally, for each estimated model, we compute the implied plug-in moments as derived in Section 2.1 when ϕ is fixed, or simulate them when ϕ changes.

Table 4 reports the posterior means and credible intervals, together with the DIC and the plug-in variance

and kurtosis, while Figs. 3 and 4 plot the plug-in autocorrelations of squares and cross-correlations. Consider first the results for S&P 500 returns. Looking at the credible intervals, all of the estimates of the CTSV1 parameters are different from zero. The estimates suggest that, on top of the significant negative correlation between the level and log-volatility noises, the threshold effect is positive

Table 4

WinBUGS posterior means and credible intervals (in parentheses) of different models fitted to daily S&P 500 and FTSE 100 returns.

		α	α_0	ϕ	$\phi + \phi_0$	γ_1	δ	σ_{η}^2	ν	DIC	Plug-in	
											Standard deviation	Kurtosis
S&P 500	CTSV1	-0.018 (-0.029, -0.007)	0.103 (0.049, 0.176)	0.961 (0.947, 0.972)	0.991 (0.977, 0.999)	-0.166 (-0.203, -0.141)	-0.906 (-0.985, -0.812)	0.011 (0.006, 0.016)	1.310 (1.130, 1.481)	6034.96	1.074	8.978
	CTSV2	-0.023 (-0.052, 0.004)	0.044 (-0.010, 0.105)	0.972 (0.958, 0.987)	0.988 (0.972, 0.999)	-0.147 (-0.176, -0.113)		0.011 (0.007, 0.016)	1.606 (1.554, 1.657)	6109.35	1.262	9.371
	A-ARSV	-0.002 (-0.006, 0.001)		0.980 (0.974, 0.984)		-0.162 (-0.187, -0.136)		0.011 (0.009, 0.015)	1.698 (1.636, 1.755)	6098.24	1.260	8.578
	TSV1	-0.122 (-0.146, -0.101)	0.259 (0.214, 0.310)	0.974 (0.960, 0.989)	0.984 (0.965, 0.997)		-0.015 (-0.029, 0.006)	0.018 (0.012, 0.025)	1.829 (1.711, 1.930)	6256.04	1.411	7.244
	TSV2	-0.110 (-0.137, -0.090)	0.231 (0.191, 0.286)	0.980 (0.967, 0.994)	0.988 (0.968, 0.999)			0.012 (0.008, 0.020)	1.331 (1.130, 1.626)	6089.34	1.489	9.430
	FTSE 100	CTSV1	-0.030 (-0.042, -0.019)	0.177 (0.111, 0.243)	0.954 (0.946, 0.963)	0.989 (0.971, 0.999)	-0.146 (-0.182, -0.108)	-0.980 (-0.997, -0.959)	0.010 (0.007, 0.015)	1.221 (1.066, 1.385)	6106.49	1.081
CTSV2		-0.015 (-0.037, 0.009)	0.028 (-0.022, 0.078)	0.970 (0.960, 0.979)	0.994 (0.985, 1.000)	-0.152 (-0.185, -0.120)		0.010 (0.007, 0.013)	1.230 (1.048, 1.485)	6149.87	1.293	13.987
A-ARSV		-0.0031 (-0.0066, 0.0003)		0.983 (0.978, 0.987)		-0.143 (-0.167, -0.122)		0.010 (0.007, 0.014)	1.800 (1.695, 1.900)	6220.45	1.247	7.864
TSV1		-0.098 (-0.126, -0.075)	0.240 (0.188, 0.301)	0.962 (0.951, 0.973)	0.994 (0.984, 1.000)		-0.174 (-0.198, -0.131)	0.015 (0.011, 0.017)	1.744 (1.700, 1.808)	6201.24	1.275	6.596
TSV2		-0.109 (-0.136, -0.085)	0.226 (0.176, 0.281)	0.970 (0.956, 0.983)	0.994 (0.981, 1.000)			0.017 (0.013, 0.025)	1.793 (1.658, 1.949)	6284.72	1.378	7.917

RETURNS

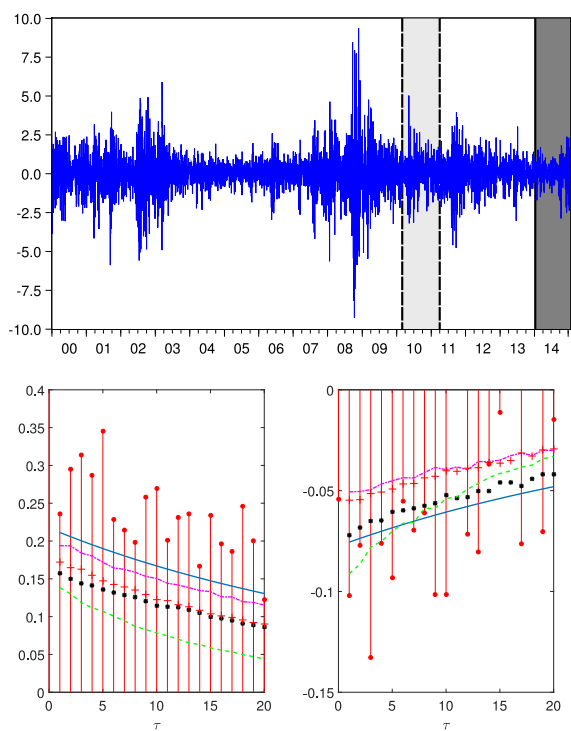


Fig. 4. The top graph displays daily FTSE 100 returns, with the vertical line indicating the start of the out-of-sample period. The two shadow areas correspond to the first (dark grey) and second (light grey) out-of-sample periods, respectively. The bottom graphs show the sample autocorrelations of squares (left) and cross-correlations of returns and future squared returns (right), together with the corresponding plug-in moments obtained after fitting the CTSV1 (green dashed lines), CTSV2 (black star-marked lines), A-ARSV (blue continuous lines), TSV1 (magenta dash-dot lines), and TSV2 (red plus-marked lines) models to the daily FTSE 100 returns.

when the standardized returns are smaller than -0.906 . With respect to persistence, Table 4 reports ϕ and $\phi + \phi_0$, which suggest that, as usual, the persistence is very close to unity in each regime. Finally, the estimated parameter

of the GED distribution suggests that the distribution of standardized returns is far from normality. Note that the DIC is minimized for the CTSV1 model with $\delta \neq 0$. When looking at the restricted specifications, we can observe that, in the CTSV2 model, $\hat{\alpha}$ and $\hat{\alpha}_0$ are hardly different from zero when $\delta = 0$, meaning that the estimates of the CTSV2 and A-ARSV parameters are very similar. Observe that their DIC values are also very similar. Furthermore, the δ parameter in the TSV1 model is not different from zero. This is why the estimated parameters of the TSV1 and TSV2 models are rather similar, except that the errors of TSV1 are closer to normality than those of the TSV2 model. The DIC of the TSV1 model is clearly the largest of all of the models fitted. The TSV1 model seems to be rejected, since it implies normality.

When looking at the standard deviation and kurtosis values implied by the estimated models, we can see that they are closer to the observed values when the CTSV2 model with $\delta = 0$ is fitted. Furthermore, Fig. 3 shows that this model generates series with autocorrelations of squares and cross-correlations that are closer to those observed for S&P 500 returns. Also note that, as would be expected given the results of the estimated parameters, the moments implied by the CTSV2 and A-ARSV models are almost identical. Finally, the TSV1 model with $\delta \neq 0$ generates values of the variance, kurtosis, autocorrelations of squares and cross-correlations which are further from the corresponding empirical moments for S&P 500 than those implied by any of the alternative models considered. After analyzing a series of daily CRSP portfolio returns, Smith (2009) also concludes that a general model dominates purely threshold and correlated models in terms of both the AIC and BIC.

The TSV1 model with $\delta \neq 0$ is clearly rejected in terms of both the DIC and the moments that it is able to represent. It seems that one needs to have some leverage around zero returns when representing the dynamic dependence of S&P 500 volatilities. Once this asymmetric effect is incorporated through the correlation between ϵ_t and η_t , a model with a threshold that is different from zero is a good compromise between the fit (measured by the DIC) and the representation of moments. Also, it seems to be important to have standardized returns with heavy tails, according

to the estimation results. Note that if the comparison is carried out between the A-ARSV and TSV2 with $\delta = 0$ models, as is usual in the literature, the evidence in favour of one model over the other is rather weak; see [Wu and Zhou \(2015\)](#), who find weak evidence in favour of the TSV model.

Finally, the volatility responses defined in Eq. (10) that are implied by different models are plotted in [Fig. 6](#). We can see that the surfaces of the models in which there is correlation are completely different from those in which $\gamma_1 = 0$.

Consider now the results for FTSE 100 returns. [Table 4](#) shows that the means of the estimated parameters of the CTSV1 model are far from zero. As for S&P 500 returns, the estimates of α and α_0 in the pure TSV models are very similar, regardless of whether $\delta = 0$ or not. However, once the γ_1 parameter is estimated, α_0 is no different from zero when $\delta = 0$. In this case, the main difference between the CTSV2 and A-ARSV models appears in the estimation of the parameter of the GED distribution, which is closer to normality in the A-ARSV model. The minimum DIC is also achieved for the CTSV1 model with $\delta \neq 0$. Note that the DIC is not very different from that of the TSV2 model with $\delta = 0$. However, the DICs of the restricted A-ARSV and TSV1 models are clearly larger. Once more, we can observe that the DICs of the models that imply standardized returns that are close to normality are clearly larger than those of the models in which ϵ_t has heavy tails.

When looking at the implied moments reported in [Table 4](#) and the implied autocorrelations of squares and cross-correlations plotted in [Fig. 4](#), we can see that the A-ARSV model represents the sample moments adequately while the TSV2 with $\delta = 0$ is far from them. When focusing on the comparison between the A-ARSV and TSV2 with $\delta = 0$ models, we can see that there is evidence in favour of the former; this conclusion is in accord with those of [Asai and McAleer \(2005\)](#), [Smith \(2009\)](#) and [Wang \(2012\)](#).

The volatility responses for FTSE 100 returns are not plotted here because they are very similar to those obtained for S&P 500 returns.

4.2. Implications for option pricing

We next analyze whether modelling the leverage effect through a threshold, as in the TSV model, or through correlation, as in the A-ARSV model, has any effect on option pricing in the context of the S&P 500 and FTSE 100 returns described above.

Consider a European call option on a stock with maturity τ (measured in the number of days). The value of the call option in terms of Black–Scholes parameters is given by

$$C(S_t, t) = N(d_1)S_t - N(d_2)Xe^{-r\tau}, \quad (11)$$

where S_t is the spot price of the underlying index at time t , $N(\cdot)$ is the cumulative distribution function of the standard normal distribution, r is the risk free rate (an annual rate, expressed in terms of continuous compounding), and X is the strike price. Finally, $d_1 = \frac{1}{\omega_\tau} \left[\ln\left(\frac{S_t}{X}\right) + \left(r - q + \frac{\sigma^2}{2}\right) \tau \right]$ and $d_2 = d_1 - \omega_\tau$ with

$\omega_\tau^2 = \int_0^\tau \exp(h_s) ds$, where q is the dividend yield and σ is the marginal standard deviation of the underlying asset returns. Since the models are estimated in discrete time, we have to approximate ω_τ^2 . In particular,

$$\hat{\omega}_\tau^2 = \sum_{t=1}^{\tau} \exp(\hat{h}_t),$$

where $\tau = 126$ is the number of days until the option matures and \hat{h}_t is the estimated log-volatility at time t . For the majority of SV models, including TSV, option prices do not have a closed form solution, meaning that the use of approximations is needed. Following [Yu et al. \(2006\)](#), we approximate option prices using Monte Carlo simulations.

We price the S&P 500 and FTSE 100 options using the parameter estimates obtained in [Section 4.1](#) and fix the risk free rates to $r = 0.08\%$ and 0.415% for S&P 500 and FTSE 100, respectively, and the dividend yield averages between 2009 and 2015 to $q = 0.0202$ and 0.0351 . We consider several ratios between the spot and strike prices; in particular, a grid of values of S_0/X between 0.75 and 1.25, with increases of 0.05. Finally, the initial value for \hat{h}_t is given by $\hat{h}_0 = \log \hat{\sigma}_0^2$, where $\hat{\sigma}_0^2$ is the sample marginal variance of returns. In particular, $\hat{\sigma}_0 = 1.280$ for S&P 500 returns, while $\hat{\sigma}_0 = 1.220$ for FTSE 100 returns. [Table 5](#) reports the option prices obtained with the different models, together with the percentage differences between each of them and the option prices obtained with the A-ARSV model. The prices obtained from the estimated A-ARSV model are smaller. The increase in prices that is observed in the threshold models when $\gamma_1 \neq 0$ is not relevant. However, there is a large increase in option prices when the prices are obtained from TSV models which do not include correlation. Therefore, it seems to be important for the specification of the asymmetric response of volatility to incorporate correlation when obtaining option prices.

4.3. Out-of-sample volatility forecasts

This section obtains one-step-ahead out-of-sample volatility forecasts. Our analysis provides a first step towards understanding the impact of the asymmetric specification on volatility forecasting. Given the extremely heavy computations that are involved in obtaining one-step-ahead volatility forecasts based on the MCMC estimator, the parameters are estimated using a rolling-window scheme with $T = 1006$ and 1042 observations for S&P 500 and FTSE 100, respectively; see [Giacomini and White \(2006\)](#) for a similar rolling window scheme with a fixed number of observations. Moreover, one-step-ahead volatilities are obtained from January 2, 2014, till January 29, 2015, with $H = 271$ and 274 out-of-sample forecasts for S&P 500 and FTSE 100, respectively. As a robustness check, we also consider two more out-of-sample periods, from December 31, 2009, to January 1, 2011, for S&P 500 returns and from February 23, 2010, till March 28, 2011, for FTSE 100 returns; see [Figs. 3 and 4](#), in which the out-of-sample periods are marked by shaded areas. Note that the first out-of-sample period considered, which corresponds to 2014, is a rather quiet period with quite a low volatility. However, the earlier out-of-sample periods, corresponding

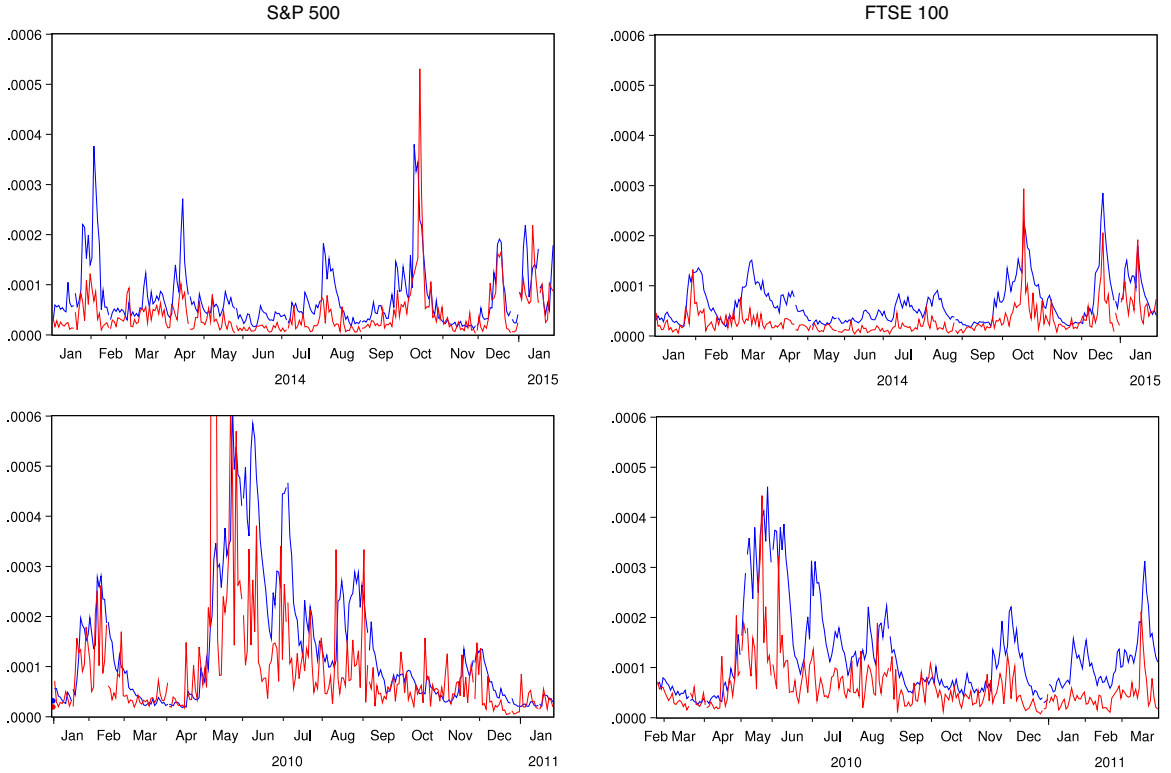


Fig. 5. Estimated volatilities of the S&P 500 and FTSE 100 daily returns. Notes: The red lines correspond to the realized volatility and the blue lines to the estimated volatilities obtained using the CTSV1 model during the first (top row) and second (bottom row) out-of-sample periods. (For interpretation of the references to colour in this figure legend, the reader is referred to the web version of this article.)

to 2010–2011, are periods of turmoil, with high volatilities. Summary statistics of the out-of-sample returns in both subperiods are reported in Table 3. We evaluate the forecasting performances of the models considered by using 5-min based realized volatilities as proxies for the true latent volatilities; see Patton (2011) for alternative volatility proxies.⁸

For each return series and out-of-sample period considered, Table 6 reports the results from the following Mincer–Zarnowitz generalized least squares (GLS) regression that is robust to noise in the volatility proxy:

$$\frac{rv_t^2}{\hat{\sigma}_{it}^2} = \frac{\beta_{0i}}{\hat{\sigma}_{it}^2} + \beta_{1i} + u_{it}, \quad (12)$$

where rv_t^2 is the realized volatility corresponding to day t and $\hat{\sigma}_{it}^2$ is the one-step-ahead forecast of the volatility corresponding to day t obtained using model i ; see Patton and Sheppard (2009), who show that the GLS regression in Eq. (12) has more power than various alternatives. The p -values reported in Table 6 correspond to the null hypotheses $\beta_0 = 0$ and $\beta_1 = 1$ and the joint test of the null $\beta_0 = 0$ and $\beta_1 = 1$. First of all, Table 6 shows that, in general, $\beta_0 > 0$ and $0 < \beta_1 < 1$, for all models, returns and subperiods considered; see Patton (2006), who

reports very similar parameter estimates in the context of forecasting the conditional variance of a series of daily IBM returns. Except for the estimate of β_0 for S&P 500 returns in the first out-of-sample period considered when the volatility is forecast using the TSV models, all of the estimates are significantly different from their hypothesized values at the 5% level. Also note that, as we would expect given the estimation results in Section 4.1, the results of the Mincer–Zarnowitz regressions for the A-ARSV and CTSV2 models are almost identical for S&P 500 returns. In any case, the estimates of the Mincer–Zarnowitz regression reported in Table 6 suggest that the volatility forecasts obtained by the asymmetric SV models considered all overestimate the corresponding realized volatilities. Fig. 5, which plots the realized volatilities together with the corresponding forecasts obtained with the general CSTV1 model for the two return series and out-of-sample periods, illustrates the overestimation of realized volatilities.

We can conclude that none of these forecasts are optimal. This conclusion leads to the question of relative forecast performances, for which we consider two widely used alternative consistent loss functions, namely the symmetric mean square forecast error (MSFE) and the QLIKE loss, which put relatively less weight on negative than positive volatility forecast errors. Note that, although the rankings obtained from consistent loss functions are invariant to noise in the volatility proxy, the actual level of expected loss obtained using a proxy is larger than that which is obtained when using the true conditional variance. Table 7

⁸ The realized volatilities have been obtained from the Realized Library of Oxford-Man Institute of Quantitative Finance (<http://realized.oxford-man.ox.ac.uk/>) as the sum of 5-min squared returns.

Table 5
S&P 500 and FTSE 100 call option prices obtained from different models for different strike prices.

	S/X	CTSV1	CTSV2	A-ARSV	TSV1	TSV2	Percentage difference vs. A-ARSV			
							CTSV1	CTSV2	TSV1	TSV2
S&P 500	0.75	1576.70	1576.67	1556.71	1766.89	1766.14	0.01	0.01	0.13	0.14
	0.8	1688.59	1616.12	1618.44	1795.51	1766.85	0.04	0.00	0.09	0.11
	0.85	1686.33	1609.33	1598.87	1806.61	1808.13	0.05	0.01	0.13	0.13
	0.9	1679.79	1682.17	1603.16	1823.97	1818.44	0.05	0.05	0.13	0.14
	0.95	1740.82	1687.39	1644.89	1838.38	1813.58	0.06	0.03	0.10	0.12
	1	1744.04	1688.78	1679.21	1829.12	1823.58	0.04	0.01	0.09	0.09
	1.05	1770.78	1709.83	1687.95	1830.83	1837.69	0.05	0.01	0.09	0.08
	1.1	1749.22	1712.70	1721.89	1871.71	1851.03	0.02	-0.01	0.07	0.09
	1.15	1788.22	1697.95	1705.03	1870.97	1864.72	0.05	0.00	0.09	0.10
	1.2	1778.29	1767.90	1711.64	1891.42	1853.54	0.04	0.03	0.08	0.11
1.25	1781.65	1750.95	1727.73	1879.55	1853.17	0.03	0.01	0.07	0.09	
FTSE 100	0.75	5994.51	5985.73	5927.58	6410.21	6262.04	0.01	0.01	0.06	0.08
	0.8	6080.35	5955.68	5908.35	6419.35	6322.69	0.03	0.01	0.07	0.09
	0.85	6010.32	6060.64	5929.66	6424.54	6382.76	0.01	0.02	0.08	0.08
	0.9	6104.27	6163.87	5964.29	6482.68	6406.81	0.02	0.03	0.07	0.09
	0.95	6130.33	6146.90	5994.75	6479.50	6406.71	0.02	0.03	0.07	0.08
	1	6185.81	6199.47	6011.87	6525.38	6445.63	0.03	0.03	0.07	0.09
	1.05	6191.97	6191.79	6141.88	6486.74	6462.11	0.01	0.01	0.05	0.06
	1.1	6247.77	6238.45	6112.04	6504.77	6424.99	0.02	0.02	0.05	0.06
	1.15	6224.33	6235.32	6175.43	6533.01	6473.05	0.01	0.01	0.05	0.06
	1.2	6299.57	6267.36	6175.78	6543.84	6473.58	0.02	0.01	0.05	0.06
1.25	6310.28	6304.61	6227.27	6563.97	6500.85	0.01	0.01	0.04	0.05	

Table 6
Results of Mincer–Zarnowitz regressions for volatility forecasts.

	Panel A					Panel B				
	CTSV1	CTSV2	A-ARSV	TSV1	TSV2	CTSV1	CTSV2	A-ARSV	TSV1	TSV2
S&P 500										
β_0	4.5×10^{-6}	5.8×10^{-6}	6.9×10^{-6}	1.3×10^{-6}	1.6×10^{-6}	2.1×10^{-5}	2.0×10^{-5}	2.0×10^{-5}	1.2×10^{-5}	1.7×10^{-5}
	(0.037)	(0.004)	(0.002)	(0.829)	(0.367)	(0.000)	(0.001)	(0.000)	(0.042)	(0.006)
β_1	0.490	0.477	0.458	0.570	0.638	0.558	0.570	0.592	0.648	0.619
	(0.000)	(0.000)	(0.000)	(0.000)	(0.000)	(0.000)	(0.000)	(0.000)	(0.001)	(0.000)
R^2	0.363	0.405	0.409	0.283	0.387	0.240	0.240	0.248	0.195	0.190
F-test	0.000	0.000	0.000	0.000	0.000	0.000	0.000	0.000	0.001	0.001
FTSE 100										
β_0	8.6×10^{-6}	9.7×10^{-6}	8.3×10^{-6}	4.0×10^{-6}	5.2×10^{-6}	1.9×10^{-6}	$\times 10^{-5}$	2.1×10^{-5}	1.9×10^{-5}	1.7×10^{-5}
	(0.000)	(0.000)	(0.000)	(0.015)	(0.001)	(0.000)	(0.000)	(0.000)	(0.000)	(0.001)
β_1	0.334	0.323	0.337	0.435	0.445	0.335	0.328	0.329	0.377	0.350
	(0.000)	(0.000)	(0.000)	(0.000)	(0.000)	(0.000)	(0.000)	(0.000)	(0.000)	(0.000)
R^2	0.498	0.315	0.489	0.501	0.435	0.406	0.431	0.435	0.367	0.359
F-test	0.000	0.000	0.000	0.000	0.000	0.000	0.000	0.000	0.000	0.000

Notes: The numbers in parentheses are p -values of the hypothesis $\beta_0 = 0$ and $\beta_1 = 1$. The F-test row reports p -values of the joint test statistic for $\beta_0 = 0$ and $\beta_1 = 1$. Panel A (B) corresponds to the first (second) out-of-sample period.

Table 7
MSFE $\times 10^9$ and mean QLIKE values for several models.

	Out-of-sample period 1				Out-of-sample period 2			
	S&P 500		FTSE 100		S&P 500		FTSE 100	
	MSE	QLIKE	MSE	QLIKE	MSE	QLIKE	MSE	QLIKE
CTSV1	3.537	0.321	2.046	0.335	20.814	0.274	8.6941	0.291
CTSV2	2.984	0.311	2.476	0.348	20.612	0.277	8.083	0.277
A-ARSV	2.899	0.312	1.973	0.339	18.991	0.275	7.889	0.265
TSV1	2.539	0.357	1.591	0.308	20.845	0.287	5.603	0.258
TSV2	1.895	0.261	1.485	0.281	21.049	0.296	7.023	0.306

reports the MSFE and the QLIKE values for each return series analyzed and each forecasting period. First of all, it is important to note that the orderings obtained using MSFE and QLIKE are rather different both from each other and from those obtained using the R^2 of the Mincer–Zarnowitz regressions. Although a common response to the concern that a few extreme observations can drive the results of volatility comparisons is to use alternative measures of the forecast accuracy, there are arguments for relying more on the QLIKE for evaluating volatility forecasts than on the more popular MSFE; see [Patton and Sheppard \(2009\)](#).

According to the QLIKE criterion, the threshold TSV2 models ranks first for S&P 500 returns in the first out-of-sample period, while the general CTSV1 model ranks first in the second out-of-sample period. Similarly, TSV2 model is ranked first for the FTSE volatility forecasts during the first-out-of-sample period, while the TSV1 model is ranked first during the second one.

Given that we are considering several models, the comparison is carried out using the model confidence set (MCS) of [Hansen, Lunde, and Nason \(2011\)](#) instead of carrying out multiple pairwise statistical comparisons of the MSFE and

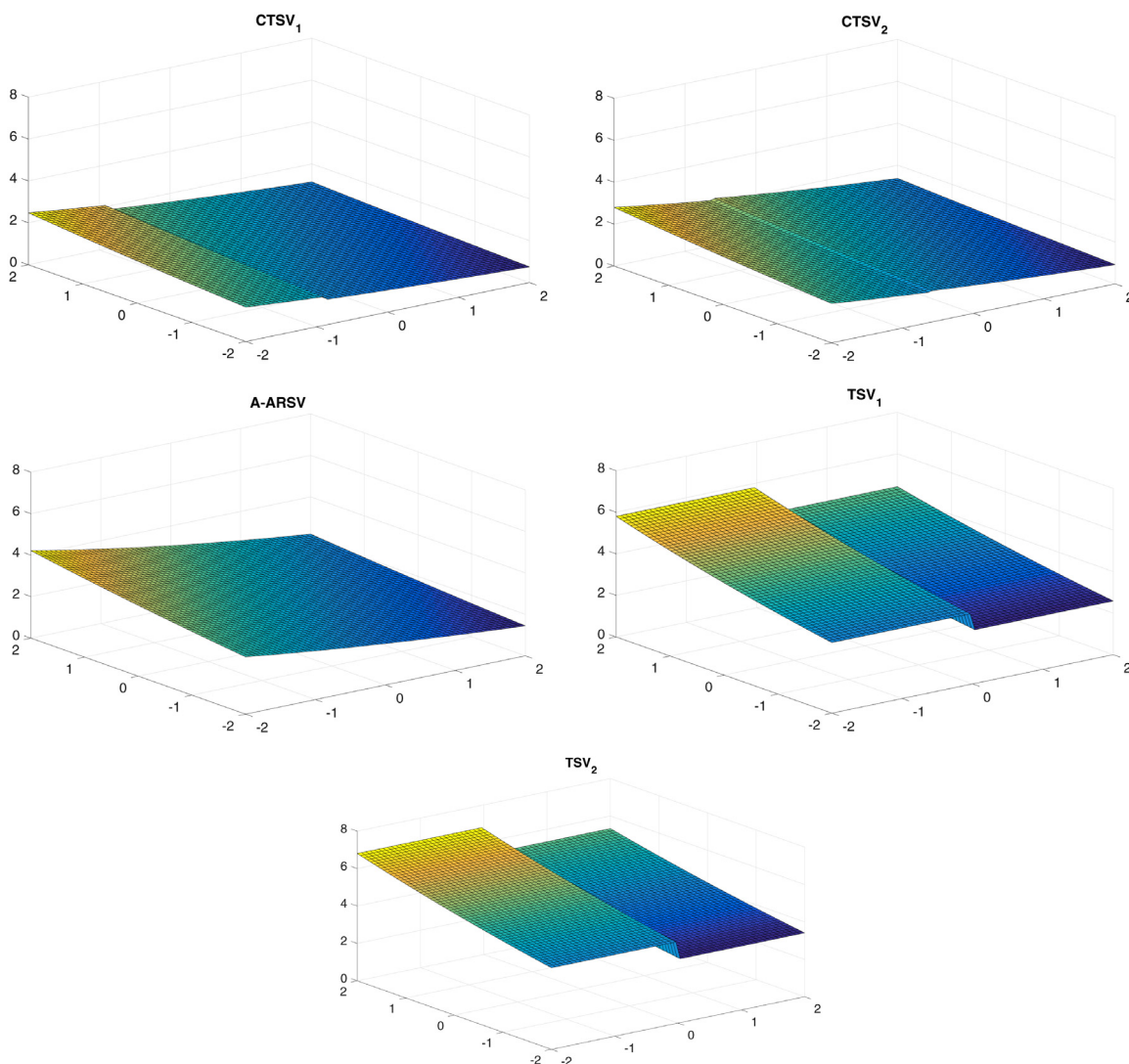


Fig. 6. Plug-in volatility surfaces obtained by fitting asymmetric SV models with different volatility specifications to S&P 500 daily returns.

Table 8
Model confidence sets.

	CTSV1	CTSV2	A-ARSV	TSV1	TSV2	<i>p</i> -value	CTSV1	CTSV2	A-ARSV	TSV1	TSV2	<i>p</i> -value
	period 1						period 2					
	S&P 500						FTSE 100					
MSFE	5**	4**	3**	2**	1**	0.999	4**	5	3**	2**	1**	0.569
QLIKE	4*	2*	3*	5**	1*	1	3**	5**	4**	2**	1**	1
	period 1						period 2					
MSFE	3**	2**	1**	4**	5**	1	5**	4**	3**	1**	2**	1
QLIKE	1**	3*	2**	4	5	0.218	4	3	2*	1**	5	0.254

Notes: Model superior sets are built based on 5,000 bootstrap samples using the MSFE and QLIKE loss functions.

* The model is in the MCS at the 10% level.

** The model is in the MCS at the 25% level.

QLIKE loss functions of the alternative models considered.⁹ The MCS procedure does not require a benchmark to be

specified, which is very useful in applications without an obvious benchmark, as is the case here. Furthermore, the MCS procedure does not assume that any particular model is the true model. Table 8 reports the orderings of the models according to the MSFE and QLIKE, together with

⁹ We use the MCS package by Leopoldo Catania and Mauro Bernardi.

information about which models are contained in the MCS with confidence level $(1 - \alpha)\%$, where $\alpha = 10\%$ and 25% .

Consider first the results for S&P 500 returns during the first (tranquil) out-of-sample period. In this case, all models are included in the MCS, regardless of the level of confidence or whether we look at the MSFE or QLIKE criteria. However, only the CTSV1 and A-ARSV models are in the MCS in the second, more volatile out-of-sample period if $\alpha = 25\%$. Similarly, when looking at the results for FTSE returns, we observe that all models are contained in the MCS in the first out-of-sample period, regardless of the criterion or confidence level. The only exception is the CTSV2 model when using the MSFE loss function. However, in the second, more volatile out-of-sample period, the only model in the MCS with a confidence of 25% is TSV1. Note that MCS should be applied with caution here because the forecasts are based on estimated parameters and some of the models are nested. However, the p -values reported in Table 8 are large enough to enable us to be confident in our conclusions. Therefore, it seems that there is only limited information available for narrowing the set of volatility forecasts considered in this paper when the comparison is carried out during tranquil volatility periods. This result is as expected, given that, as was mentioned above, the volatility responses of asymmetric SV models are weaker when the volatility noise is negative and, consequently, the volatility is below average. Therefore, we expect a weak leverage effect in periods of low volatility, with negative shocks to the volatility. In these periods, the particular specification that is adopted for the leverage could be less important. Furthermore, the QLIKE loss seems to be more informative for comparing alternative forecasts, especially in the high volatility periods. With respect to the particular specifications chosen in the second out-of-sample period considered, models with thresholds that are different from zero are always in the MCS. Whether the model also incorporates leverage through correlation or not depends on the particular series of returns analyzed. The problem of instability in the performances and predictive content of different forecasting methods is well known, and is surveyed by Rossi (2013).

Finally, it is remarkable that models that imply similar autocorrelations of squares and cross-correlations between returns and future squared returns are also ranked similarly when forecasting volatilities out-of-sample. This is the case for S&P 500 returns. Fig. 3 shows that the CTSV2 and A-ARSV models imply very similar autocorrelations and cross-correlations, and the rankings of these two models in our out-of-sample comparison are very close.

5. Conclusion

This paper analyzes the ability of TSV models to explain the empirical properties that are often observed when dealing with financial returns, and to forecast volatilities. The TSV models considered in this paper allow the threshold parameter to be different from zero. We derive the statistical properties of the TSV model when the level errors are assumed to be GED. If the threshold persistence parameter is different from zero, the properties are analyzed by simulation. We show that changes in the variance

of the log-volatility disturbance depending on the sign of past returns do not generate a leverage effect. However, changing the constant in the volatility equation allows the model to capture asymmetric conditional heteroscedasticity. Furthermore, changes in the persistence parameter add flexibility to the TSV model that is able to generate returns with kurtoses and autocorrelations of squared returns similar to those that are often observed when dealing with real time series of financial returns. We compare the properties of the TSV model with those of the popular A-ARSV model and show that, although both models are able to generate series with conditional heteroscedasticity and leverage, the TSV models generate slightly less leverage than the A-ARSV model. We also consider models in which leverage is incorporated by both correlation and the threshold parameters.

Our second contribution is to show that the MCMC estimator of WinBUGS has good properties for estimating the parameters of the CTSV model which nests both the TSV and A-ARSV models. We show that the MCMC estimator is able to discriminate between the two specifications, and also allows us to obtain volatility forecasts.

Finally, we compare the models empirically in terms of their in-sample fits, plug-in moments and pricings of European options. The CTSV model performs best in-sample for the fit and moments. We also show that different specifications of the asymmetric volatilities generate rather different European option prices. The option prices generated by TSV are larger than those obtained in models that also incorporate leverage through the correlation between the level and volatility noises. We also compare their out-of-sample abilities for forecasting the volatility. For the out-of-sample forecasts, none of the models clearly emerges as best. In the absence of a strong, consistent forecast accuracy advantage of one model over another, one might argue that the specification with a better match of moments is preferable conceptually. Overall, it seems that models in which leverage is incorporated by both threshold variables and correlated errors can be a good compromise.

Acknowledgments

We acknowledge financial support from the Spanish Ministry of Economy and Competitiveness, research projects ECO2015-70331-C2-2-R and ECO2015-65701-P, as well as FCT grant UID/GES/00315/2013. We are also very grateful to Rutger Lit for helpful comments on the estimation of asymmetric stochastic volatility models, to Jesus Gonzalo for discussions on threshold autoregressive models, and to two anonymous reviewers and an Associate Editor for helpful comments that improved this paper.

Appendix A. Properties of the CTSV model

Consider the general CTSV model given by Eqs. (1), (3) and (4) with $\phi_0 = 0$. The log-volatility, h_t , can be written as

$$h_t = \sum_{i=1}^{\infty} \phi^{i-1} f(\epsilon_{t-i}, \eta_{t-i}; \theta). \quad (\text{A.1})$$

A.1. Stationarity of y_t

Note that, by definition, $\text{Var}(f(\epsilon_t, \eta_t; \theta)) < \infty$. Furthermore, if $|\phi| < 1$ then $\sum_{i=1}^{\infty} \phi^{2i-2} < \infty$, and it can be shown, following the proof in Appendix A.1 of Mao et al. (2015), that y_t is strictly stationary and ergodic. In addition, $\sigma_t^2 = \exp(h_t)$ is also strictly stationary. Consequently, any existing moments of y_t and σ_t^2 are time invariant.

A.2. Moments of y_t

Consider a nonnegative finite integer c . From Eq. (A.1), the power-transformed volatility can be written as

$$\sigma_t^c = \exp\left(0.5c \sum_{i=0}^{\infty} \phi^i f(\epsilon_{t-i-1}, \eta_{t-i-1}; \theta)\right). \quad (\text{A.2})$$

Given that ϵ_t and η_t are mutually independent for all lags and leads, after taking expectations on both sides of Eq. (A.2) we obtain

$$E(\sigma_t^c) = \prod_{i=0}^{\infty} E\left[\exp(0.5c\phi^i f(\epsilon_{t-i-1}, \eta_{t-i-1}; \theta))\right]. \quad (\text{A.3})$$

If $|\phi| < 1$, then $E(\sigma_t^c)$ is finite; see Mao et al. (2015, Appendix A.1). Furthermore, taking into account the fact that η_t has a standardized normal distribution, and denoting $a = 0.5c\phi^i$, the expectation in Eq. (A.3) is given by

$$\begin{aligned} & E(\exp(af(\epsilon, \eta; \theta))) \\ &= \text{Prob}(\epsilon \geq \delta)E(\exp(a\alpha + a\gamma_1\epsilon + a\sigma_\eta\eta)|\epsilon \geq \delta) \\ &\quad + \text{Prob}(\epsilon < \delta)E(\exp(a(\alpha + \alpha_0) \\ &\quad + a\gamma_1\epsilon + a(\sigma_\eta + \sigma_{\eta_0})\eta)|\epsilon < \delta) \\ &= \text{Prob}(\epsilon \geq \delta)E(\exp(a\gamma_1\epsilon)|\epsilon \geq \delta) \exp\left(a \cdot \frac{a\sigma_\eta^2 + 2\alpha}{2}\right) \\ &\quad + \text{Prob}(\epsilon < \delta)E(\exp(a\gamma_1\epsilon)|\epsilon < \delta) \\ &\quad \times \exp\left(a \cdot \frac{a(\sigma_\eta + \sigma_{\eta_0})^2 + 2(\alpha + \alpha_0)}{2}\right). \end{aligned} \quad (\text{A.4})$$

Finally, given that σ_t and ϵ_t are contemporaneously independent, we obtain the expectation

$$E(y_t^c) = E(\sigma_t^c)E(\epsilon_t^c). \quad (\text{A.5})$$

Furthermore, if ϵ_t is such that $E(\epsilon_t^c) < \infty$, then y_t will have finite moments of arbitrary order c .

A.3. Autocorrelations of y_t^c

Note that, for $r = 1, 2, \dots$, we can write σ_t^c as

$$\sigma_t^c = \exp\left\{0.5c \sum_{i=1}^r \phi^{i-1} f(\epsilon_{t-i}, \eta_{t-i}; \theta)\right\} \sigma_{t-r}^{c\phi^r}, \quad (\text{A.6})$$

and consequently, the following expression of the autocovariance is obtained:

$$\begin{aligned} & \text{cov}(y_t^c, y_{t-r}^c) \\ &= E\left(\epsilon_t^c \epsilon_{t-r}^c \exp\left(\sum_{i=1}^r 0.5c\phi^{i-1} f(\epsilon_{t-i}, \eta_{t-i}; \theta)\right) \sigma_{t-r}^{c(\phi^r+1)}\right) \\ &\quad - \left\{E(\epsilon_t^c) E(\sigma_t^c)\right\}^2. \end{aligned} \quad (\text{A.7})$$

Given that ϵ_t and η_t are iid sequences that are mutually independent for any lag and lead, and that σ_{t-r} depends only on lagged disturbances, substituting Eq. (A.3) into Eq. (A.7) gives

$$\begin{aligned} & \text{cov}(y_t^c, y_{t-r}^c) \\ &= E(\epsilon_t^c) E(\epsilon_{t-r}^c \exp(0.5c\phi^{r-1} f(\epsilon_t, \eta_t; \theta))) \\ &\quad \times \prod_{i=1}^{r-1} E(\exp(0.5c\phi^{i-1} f(\epsilon_{t-i}, \eta_{t-i}; \theta))) \\ &\quad \times P(0.5c(1 + \phi^r), \phi) \\ &\quad - (E(\epsilon_t^c))^2 [E(\sigma_t^c)]^2, \end{aligned}$$

where $E(\exp(0.5c\phi^{i-1} f(\epsilon_{t-i}, \eta_{t-i}; \theta)))$ and $P(0.5c(1 + \phi^r), \phi) = \prod_{i=1}^{\infty} E(\exp(0.5c(1 + \phi^r)\phi^{i-1} f(\epsilon_{t-i}, \eta_{t-i}; \theta)))$ can be obtained from Eq. (A.4) by changing the constant a adequately.

The required expression of $\rho_c(r)$ follows directly from $\rho_c(r) = \frac{\text{cov}(y_t^c, y_{t-r}^c)}{E(y_t^{2c}) - [E(y_t^c)]^2}$, where the denominator can be obtained from Eq. (A.5).

A.4. Cross-correlation between y_t^c and y_{t-r} for $r > 0$

The calculation of the cross-covariance between y_t^c and y_{t-r} is obtained by following the same steps as in A.3; that is,

$$\begin{aligned} & \text{cov}(y_t^c, y_{t-r}) \\ &= E(\epsilon_t^c) E(\epsilon_{t-r} \exp(0.5c\phi^{r-1} f(\epsilon_t, \eta_t; \theta))) \\ &\quad \times \prod_{i=1}^{r-1} E(\exp(0.5c\phi^{i-1} f(\epsilon_{t-i}, \eta_{t-i}; \theta))) \\ &\quad \times P(0.5(1 + c\phi^r), \phi). \end{aligned} \quad (\text{A.8})$$

Finally, $\rho_{c1}(r) = \frac{\text{cov}(y_t^c, y_{t-r})}{\sqrt{E(y_t^{2c}) - E^2(y_t^c)} \sqrt{E(y_{t-r}^2)}}$, where the denominator can be obtained from Eq. (A.5).

Appendix B. Derivations of probabilities, expectations and integrals when $\epsilon \sim \text{GED}(\nu)$

If ϵ has a centered and standardized GED distribution, with parameter $0 < \nu \leq \infty$, then its density function is given by $\psi(\epsilon) = C_0 \exp\left(-\frac{|\epsilon|^\nu}{2\lambda^\nu}\right)$, where $C_0 \equiv \frac{\nu}{\lambda^{2+1/\nu} \Gamma(1/\nu)}$ and $\lambda \equiv (2^{-2/\nu} \Gamma(1/\nu) / \Gamma(3/\nu))^{1/2}$, with $\Gamma(\cdot)$ being the gamma function.

B.1. Derivation of $\text{Prob}(\epsilon \geq \delta)$

Given that the GED density is symmetric, $\text{Prob}(\epsilon \geq \delta) = 0.5$ if $\delta = 0$. If $\delta > 0$, then

$$\begin{aligned} \text{Prob}(\epsilon \geq \delta) &= \int_{\delta}^{+\infty} C_0 \exp\left(-\frac{|\epsilon|^\nu}{2\lambda^\nu}\right) d\epsilon \\ &= \int_{\frac{\delta^\nu}{2\lambda^\nu}}^{+\infty} C_0 \exp(-s) 2^{1/\nu} \frac{1}{\nu} s^{1/\nu-1} \lambda ds \\ &= \frac{1}{2\Gamma(1/\nu)} \left(\frac{1}{\nu}, \frac{\delta^\nu}{2\lambda^\nu}\right), \end{aligned}$$

$$E(\epsilon^c \exp(b\gamma_1 \epsilon) | \epsilon \geq \delta) = \begin{cases} \frac{C_0}{P(\epsilon \geq \delta)} \int_{\delta}^{+\infty} |\epsilon|^c \exp(b\gamma_1 \epsilon) \exp\left(-\frac{|\epsilon|^\nu}{2\lambda^\nu}\right) d\epsilon, & \delta \geq 0 \\ \frac{C_0}{P(\epsilon \geq \delta)} (-1)^c \left\{ \int_{\delta}^0 |\epsilon|^c \exp(b\gamma_1 \epsilon) \exp\left(-\frac{|\epsilon|^\nu}{2\lambda^\nu}\right) d\epsilon + \int_0^{+\infty} |\epsilon|^c \exp(b\gamma_1 \epsilon) \exp\left(-\frac{|\epsilon|^\nu}{2\lambda^\nu}\right) d\epsilon \right\}, & \delta < 0, \end{cases}$$

and

$$E(\epsilon^c \exp(b\gamma_1 \epsilon) | \epsilon < \delta) = \begin{cases} \frac{C_0}{P(\epsilon < \delta)} \left\{ \int_0^{\delta} |\epsilon|^c \exp(b\gamma_1 \epsilon) \exp\left(-\frac{|\epsilon|^\nu}{2\lambda^\nu}\right) d\epsilon + (-1)^c \int_{-\infty}^0 |\epsilon|^c \exp(b\gamma_1 \epsilon) \exp\left(-\frac{|\epsilon|^\nu}{2\lambda^\nu}\right) d\epsilon \right\}, & \delta \geq 0 \\ (-1)^c \frac{C_0}{P(\epsilon < \delta)} \int_{-\infty}^{\delta} |\epsilon|^c \exp(b\gamma_1 \epsilon) \exp\left(-\frac{|\epsilon|^\nu}{2\lambda^\nu}\right) d\epsilon, & \delta < 0. \end{cases}$$

Box III.

where (α, x) is the upper incomplete gamma function defined as $(\alpha, x) = \int_x^{+\infty} e^{-t} t^{\alpha-1} dt$; see Ryzhik, Jeffrey, and Zwillinger (2007, formula 3.381.3). Finally, if $\delta < 0$,

$$\begin{aligned} Prob(\epsilon \geq \delta) &= \int_{\delta}^{+\infty} C_0 \exp\left(-\frac{|\epsilon|^\nu}{2\lambda^\nu}\right) d\epsilon \\ &= \int_{\delta}^0 C_0 \exp\left(-\frac{|\epsilon|^\nu}{2\lambda^\nu}\right) d\epsilon + \frac{1}{2} \\ &= \int_0^{\frac{(-\delta)^\nu}{2\lambda^\nu}} C_0 \exp(-s) 2^{1/\nu} \frac{1}{\nu} s^{1/\nu-1} \lambda ds + \frac{1}{2} \\ &= \frac{1}{2\Gamma(1/\nu)} \gamma\left(\frac{1}{\nu}, \frac{(-\delta)^\nu}{2\lambda^\nu}\right) + \frac{1}{2}, \end{aligned}$$

where $\gamma(\alpha, x)$ is the lower incomplete gamma function defined as $\gamma(\alpha, x) = \int_0^x e^{-t} t^{\alpha-1} dt$; see Ryzhik et al. (2007, formula 3.381.1).

B.2. Derivation of $E(\epsilon^c \exp(bf(\epsilon, \eta; \theta)))$ for a real number b and a nonnegative finite integer c , when $f(\epsilon, \eta; \theta)$ is given by Eq. (4), $\epsilon \sim GED(\nu)$ and $\eta \sim N(0, \sigma_\eta^2)$

$$\begin{aligned} E(\epsilon^c \exp(bf(\epsilon, \eta; \theta))) &= Prob(\epsilon \geq \delta) E(\epsilon^c \exp(b\gamma_1 \epsilon) | \epsilon \geq \delta) \\ &\quad \times \exp\left(b \cdot \frac{b\sigma_\eta^2 + 2\alpha}{2}\right) \\ &+ Prob(\epsilon < \delta) E(\epsilon^c \exp(b\gamma_1 \epsilon) | \epsilon < \delta) \\ &\quad \times \exp\left(b \cdot \frac{b(\sigma_\eta + \sigma_{\eta_0})^2 + 2(\alpha + \alpha_0)}{2}\right), \end{aligned} \quad (B.1)$$

where $Prob(\epsilon \geq \delta)$ is given in Appendix B.1, and $E(\epsilon^c \exp(b\gamma_1 \epsilon) | \epsilon \geq \delta)$ and $E(\epsilon^c \exp(b\gamma_1 \epsilon) | \epsilon < \delta)$ are given in Box III.

The integrals needed to compute these expectations are derived next:

$$\begin{aligned} &\int_0^{+\infty} |\epsilon|^c \exp(b\gamma_1 \epsilon) \exp\left(-\frac{|\epsilon|^\nu}{2\lambda^\nu}\right) d\epsilon \\ &= \int_0^{+\infty} \lambda^c 2^{\frac{c}{\nu}} y^{\frac{c}{\nu}} \exp(b\gamma_1 \lambda 2^{1/\nu} y^{1/\nu}) \end{aligned}$$

$$\begin{aligned} &\times \exp(-y) \frac{\lambda 2^{1/\nu}}{\nu} y^{1/\nu-1} dy \\ &= \frac{1}{\nu} 2^{\frac{c+1}{\nu}} \lambda^{c+1} \sum_{k=0}^{\infty} \frac{(b\gamma_1 \lambda 2^{1/\nu})^k}{k!} \int_0^{+\infty} y^{\frac{c+1+k}{\nu}-1} \\ &\quad \times \exp(-y) dy \\ &= \frac{1}{\nu} 2^{\frac{c+1}{\nu}} \lambda^{c+1} \sum_{k=0}^{\infty} \frac{(b\gamma_1 \lambda 2^{1/\nu})^k}{k!} \Gamma\left(\frac{c+1+k}{\nu}\right) \end{aligned}$$

and

$$\begin{aligned} &\int_{-\infty}^0 |\epsilon|^c \exp(b\gamma_1 \epsilon) \exp\left(-\frac{|\epsilon|^\nu}{2\lambda^\nu}\right) d\epsilon \\ &= \int_0^{+\infty} |\epsilon|^c \exp(-b\gamma_1 \epsilon) \exp\left(-\frac{|\epsilon|^\nu}{2\lambda^\nu}\right) d\epsilon \\ &= \frac{1}{\nu} 2^{\frac{c+1}{\nu}} \lambda^{c+1} \sum_{k=0}^{\infty} \frac{(-b\gamma_1 \lambda 2^{1/\nu})^k}{k!} \Gamma\left(\frac{c+1+k}{\nu}\right). \end{aligned}$$

Furthermore, when $\delta > 0$

$$\begin{aligned} &\int_{\delta}^{+\infty} |\epsilon|^c \exp(b\gamma_1 \epsilon) \exp\left(-\frac{|\epsilon|^\nu}{2\lambda^\nu}\right) d\epsilon \\ &= \int_{\frac{\delta^\nu}{2\lambda^\nu}}^{+\infty} \lambda^c 2^{\frac{c}{\nu}} y^{\frac{c}{\nu}} \exp(b\gamma_1 \lambda 2^{1/\nu} y^{1/\nu}) \\ &\quad \times \exp(-y) \frac{\lambda 2^{1/\nu}}{\nu} y^{1/\nu-1} dy \\ &= \frac{1}{\nu} 2^{\frac{c+1}{\nu}} \lambda^{c+1} \sum_{k=0}^{\infty} \frac{(b\gamma_1 \lambda 2^{1/\nu})^k}{k!} \left(\frac{c+1+k}{\nu}, \frac{\delta^\nu}{2\lambda^\nu}\right) \end{aligned}$$

and

$$\begin{aligned} &\int_0^{\delta} |\epsilon|^c \exp(b\gamma_1 \epsilon) \exp\left(-\frac{|\epsilon|^\nu}{2\lambda^\nu}\right) d\epsilon \\ &= \int_0^{\frac{\delta^\nu}{2\lambda^\nu}} \lambda^c 2^{\frac{c}{\nu}} y^{\frac{c}{\nu}} \exp(b\gamma_1 \lambda 2^{1/\nu} y^{1/\nu}) \\ &\quad \times \exp(-y) \frac{\lambda 2^{1/\nu}}{\nu} y^{1/\nu-1} dy \\ &= \frac{1}{\nu} 2^{\frac{c+1}{\nu}} \lambda^{c+1} \sum_{k=0}^{\infty} \frac{(b\gamma_1 \lambda 2^{1/\nu})^k}{k!} \gamma\left(\frac{c+1+k}{\nu}, \frac{\delta^\nu}{2\lambda^\nu}\right). \end{aligned}$$

When $\delta < 0$, the integrals required are

$$\begin{aligned} & \int_{\delta}^0 |\epsilon|^c \exp(b\gamma_1\epsilon) \exp\left(-\frac{|\epsilon|^\nu}{2\lambda^\nu}\right) d\epsilon \\ &= \int_0^{-\delta} |\epsilon|^c \exp(-b\gamma_1\epsilon) \exp\left(-\frac{|\epsilon|^\nu}{2\lambda^\nu}\right) d\epsilon \\ &= \frac{1}{\nu} 2^{\frac{c+1}{\nu}} \lambda^{c+1} \sum_{k=0}^{\infty} \frac{(-b\gamma_1\lambda 2^{1/\nu})^k}{k!} \gamma\left(\frac{c+1+k}{\nu}, \frac{(-\delta)^\nu}{2\lambda^\nu}\right) \end{aligned}$$

and

$$\begin{aligned} & \int_{-\infty}^{\delta} |\epsilon|^c \exp(b\gamma_1\epsilon) \exp\left(-\frac{|\epsilon|^\nu}{2\lambda^\nu}\right) d\epsilon \\ &= \int_{-\delta}^{+\infty} |\epsilon|^c \exp(-b\gamma_1\epsilon) \exp\left(-\frac{|\epsilon|^\nu}{2\lambda^\nu}\right) d\epsilon \\ &= \frac{1}{\nu} 2^{\frac{c+1}{\nu}} \lambda^{c+1} \sum_{k=0}^{\infty} \frac{(-b\gamma_1\lambda 2^{1/\nu})^k}{k!} \gamma\left(\frac{c+1+k}{\nu}, \frac{(-\delta)^\nu}{2\lambda^\nu}\right). \end{aligned}$$

Finally, note that $E(\epsilon^c)$ and $E(\exp(bf(\epsilon, \eta; \theta)))$ can be obtained from Eq. (B.1) by making $b = 0$ and $c = 0$, respectively.

References

Asai, M., & McAleer, M. (2004). Dynamic leverage and threshold effects in stochastic volatility models, Unpublished Manuscript, Faculty of Economics, Tokyo Metropolitan University.

Asai, M., & McAleer, M. (2005). Dynamic asymmetric leverage in stochastic volatility models. *Econometric Reviews*, 24(3), 317–332.

Asai, M., & McAleer, M. (2011). Alternative asymmetric stochastic volatility models. *Econometric Reviews*, 30, 548–564.

Berg, A., Meyer, R., & Yu, J. (2004). Deviance information criterion for comparing stochastic volatility models. *Journal of Business and Economic Statistics*, 22(1), 107–120.

Black, F. (1976). Studies of stock price volatility changes. In *Proceedings of the 1976 meeting of the business and economic statistics section* (pp. 177–191). Washington D.C.: American Statistical Association.

Breidt, F.J. (1996). A threshold autoregressive stochastic volatility model. In *VI Latin American congress of probability and mathematical statistics (CLAPEM)*, Valparaiso, Chile.

Brooks, C., Henry, O. T., & Persaud, G. (2002). The effect of asymmetries on optimal hedge ratios. *Journal of Business*, 75(2), 333–352.

Brooks, C., & Persaud, G. (2003). The effect of asymmetries on stock index return Value-at-Risk estimates. *The Journal of Risk Finance*, 4(2), 29–42.

Chen, C., Liu, F., & So, M. (2008). Heavy-tailed-distributed threshold stochastic volatility models in financial time series. *Australian and New Zealand Journal of Statistics*, 50(1), 29–51.

Chen, C., Liu, F., & So, M. (2013). Threshold variable selection of asymmetric stochastic volatility models. *Computational Statistics*, 28(6), 2415–2447.

Chen, C. W., So, M. K., & Liu, F.-C. (2011). A review of threshold time series models in finance. *Statistics and Its Interface*, 4(2), 167–181.

Christie, A. A. (1982). The stochastic behavior of common stock variances: Value, leverage and interest rate effects. *Journal of Financial Economics*, 10(4), 407–432.

Clark, P. K. (1973). A subordinated stochastic process model with finite variance for speculative prices. *Econometrica*, 41(1), 135–155.

Delatola, E.-I., & Griffin, J. E. (2013). A Bayesian semiparametric model for volatility with a leverage effect. *Computational Statistics & Data Analysis*, 60, 97–110.

Demos, A. (2002). Moments and dynamic structure of a time-varying parameter stochastic volatility in mean model. *The Econometrics Journal*, 5(2), 345–357.

Diop, A., & Guegan, D. (2004). Tail behaviour of a threshold autoregressive stochastic volatility model. *Extremes*, 7, 367–375.

Elliott, R., Liew, C., & Siu, T. (2011). On filtering and estimation of a threshold stochastic volatility model. *Applied Mathematics and Computation*, 218(1), 61–75.

Fan, T.-H., & Wang, Y.-F. (2013). An empirical Bayesian forecast in the threshold stochastic volatility models. *Journal of Statistical Computation and Simulation*, 83(3), 486–500.

Fridman, M., & Harris, L. (1998). A maximum likelihood approach for non-Gaussian stochastic volatility models. *Journal of Business and Economic Statistics*, 16(3), 284–291.

García-centeno, M. d. C., & Mínguez-Salido, R. (2009). Estimation of asymmetric stochastic volatility models for stock-exchange index returns. *International Advances in Economic Research*, 15(1), 71–87.

Ghosh, H., Gurung, B., & Source, P. (2015). Kalman filter-based modelling and forecasting of stochastic volatility with threshold. *Journal of Applied Statistics*, 42(3), 492–507.

Giacomini, R., & White, H. (2006). Tests of conditional predictive ability. *Econometrica*, 74(6), 1545–1578.

Hansen, P. R., Lunde, A., & Nason, J. M. (2011). The model confidence set. *Econometrica*, 79, 456–497.

Harvey, A. (1990). *The econometric analysis of time series* (2nd Ed.). Cambridge: MIT Press.

Harvey, A. C., & Shephard, N. (1996). Estimation of an asymmetric stochastic volatility model for asset returns. *Journal of Business and Economic Statistics*, 14(4), 429–434.

Jensen, M. J., & Maheu, J. M. (2014). Estimating a semiparametric asymmetric stochastic volatility model with a Dirichlet process mixture. *Journal of Econometrics*, 178, 523–538.

Kitagawa, G. (1987). Non-Gaussian state-space modeling of nonstationary time series. *Journal of the American Statistical Association*, 82(400), 1032–1041.

Koopman, S. J., Lucas, A., & Scharth, M. (2015). Numerically accelerated importance sampling for nonlinear non-Gaussian state space models. *Journal of Business and Economic Statistics*, 33(1), 114–127.

Li, Y., Zeng, T., & Yu, J. (2014). Robust deviance information criterion for latent variable models, CAFE Research Paper (13.19).

Lien, D. (2005). A note on asymmetric stochastic volatility and futures hedging. *Journal of Futures Markets*, 25(6), 607–612.

Liu, Q., Wong, L., An, Y., & Zhang, J. (2014). Asymmetric information and volatility forecasting in commodity futures markets. *Pacific-Basin Finance Journal*, 26, 79–97.

Mao, X., Ruiz, E., Veiga, H., & Czellar, V. (2015). Asymmetric stochastic volatility models: Properties and estimation. Available At SSRN 2544473.

Meyer, R., & Yu, J. (2000). BUGS for a Bayesian analysis of stochastic volatility models. *The Econometrics Journal*, 3(2), 198–215.

Montero-Lorenzo, J., Fernández-Avilés, G., & García-centeno, M. (2010). Estimation of asymmetric stochastic volatility models: Application to daily average prices of energy products. *International Statistical Review*, 78(3), 330–347.

Montero-Lorenzo, J., García-centeno, M., & Fernández-Avilés, G. (2011). A threshold autoregressive asymmetric stochastic volatility strategy to alert of violations of the air quality standards. *International Journal of Environmental Research*, 5(1), 23–32.

Muñoz, M. P., Marquez, M. D., & Acosta, L. M. (2007). Forecasting volatility by means of threshold models. *Journal of Forecasting*, 26(5), 343–363.

Pardo, A., & Torro, H. (2007). Trading with asymmetric volatility spillovers. *Journal of Business Finance and Accounting*, 34(9–10), 1548–1568.

Patton, A. J. (2006). Volatility forecast comparison using imperfect volatility proxies, Research Paper 175, Quantitative Finance Research Center, University of Technology Sydney.

Patton, A. J. (2011). Data-based ranking of realised volatility estimators. *Journal of Econometrics*, 161(2), 284–303.

Patton, A. J., & Sheppard, K. (2009). Evaluating volatility and correlation forecasts. In T. Mikosch, J.-P. Kreiß, R. A. Davis, & T. G. Andersen (Eds.), *Handbook of financial time series* (pp. 801–838). Berlin, Heidelberg: Springer Berlin Heidelberg.

Pérez, A., Ruiz, E., & Veiga, H. (2009). A note on the properties of power-transformed returns in long-memory stochastic volatility models with leverage effect. *Computational Statistics & Data Analysis*, 53(10), 3593–3600.

Rossi, B. (2013). Exchange rate predictability. *Journal of Economic Surveys*, 51(4), 1063–1119.

- Ruiz, E., & Veiga, H. (2008). Modelling long-memory volatilities with leverage effect: A-LMSV versus FIEGARCH. *Computational Statistics & Data Analysis*, 52(6), 2846–2862.
- Ryzhik, I., Jeffrey, A., & Zwillinger, D. (2007). *Table of integrals, series and products* (7th Ed.). London: Academic Press.
- Skaug, H. J., & Yu, J. (2014). A flexible and automated likelihood based framework for inference in stochastic volatility models. *Computational Statistics & Data Analysis*, 76, 642–654.
- Smith, D. (2009). Asymmetry in stochastic volatility models: Threshold or correlation? *Studies in Nonlinear Dynamics and Econometrics*, 13(3).
- So, M., & Choi, C. Y. (2008). A multivariate threshold stochastic volatility model. *Mathematics and Computers in Simulation*, 79(3), 306–317.
- So, M., & Choi, C. Y. (2009). A threshold factor multivariate stochastic volatility model. *Journal of Forecasting*, 28(8), 712–735.
- So, M., Li, W., & Lam, K. (2002). A threshold stochastic volatility model. *Journal of Forecasting*, 21(7), 473–500.
- Taylor, S. (2007). *Asset price dynamics, volatility, and prediction*. Princeton, NJ: Princeton University Press.
- Taylor, S. J. (1994). Modelling stochastic volatility: A review and comparative study. *Mathematical Finance*, 4, 183–204.
- Tsai-Hung, F., & Wang, Y.-F. (2013). An empirical Bayesian forecast in the threshold stochastic volatility models. *Journal of Statistical Computation and Simulation*, 83(3), 486–500.
- Vuong, Q. H. (1989). Likelihood ratio tests for model selection and non-nested hypotheses. *Econometrica*, 57(2), 307–333.
- Wang, J. J. (2012). On asymmetric generalised t stochastic volatility models. *Mathematics and Computers in Simulation*, 82(11), 2079–2095.
- Wang, J. J., Chan, J. S., & Choy, S. B. (2013). Modelling stochastic volatility using generalized t distribution. *Journal of Statistical Computation and Simulation*, 83, 340–354.
- Wirjanto, T., Kolkiewicz, A., & Men, Z. (2016). Bayesian analysis of a threshold stochastic volatility model. *Journal of Forecasting*, 35(5), 462–476.
- Wu, X.-Y., & Zhou, H.-L. (2015). A triple-threshold leverage stochastic volatility model. *Studies in Nonlinear Dynamics and Econometrics*, 19(4), 483–500.
- Xu, D. (2010). A threshold stochastic volatility model with realized volatility.
- Xu, D. (2012). Examining realized volatility regimes under a threshold stochastic volatility model. *International Journal of Finance and Economics*, 17(4), 373–389.
- Yu, J. (2012). A semiparametric stochastic volatility model. *Journal of Econometrics*, 167(2), 473–482.
- Yu, J., Yang, Z., & Zhang, X. (2006). A class of nonlinear stochastic volatility models and its implications for pricing currency options. *Computational Statistics & Data Analysis*, 51(4), 2218–2231.